FHR Code Benchmarking White Paper Series, Integrated Research Project 2, Workshop 2

Nuclear Energy University Programs

U.S. Department of Energy

Fluoride-Salt-Cooled, High-Temperature Reactor Code Benchmarking White Paper – Thermal Hydraulics Working Group

Panel Members (U.S.)

Emilio Baglietto (MIT)
Edward Blandford (UNM)
Nicholas Brown (ORNL)
Robert Budnitz (LBL)
Dave Carpenter (MIT)
Tommy Cisneros(Terrapower)
Cristian Contescu (ORNL)
Adrien Couet (UW)
Ben Forget (MIT)
Charles Forsberg (MIT)
Max Fratoni (UCB)
David Holcomb (ORNL)
Rui Hu (ANL)
Lin-wen Hu (MIT)
Steve Krahn (Vanderbilt)
Diana Li (DOE-NE)
Digby McDonald (UCB)
Cecil Parks (ORNL)
Per Peterson (UCB)
Robert Petroski (Terrapower)
Bojan Petrovic (GT)
Jeff Powers (ORNL)
Cristian Rabiti (INL)
Farzad Rahnema (GT)
Raluca Scarlat (UW)
Kumar Sridharan (UW)
Gerhard Strydom (INL)
Xiaodong Sun (OSU0
Yixing Sung (Westinghouse)
Jinsuo Zhang (OSU)

Panel Members (International)

Adrien Bidaud (Grenoble IT)
Kun Chen (SINAP)
Veronique Ghetta (Grenoble IT)
Boris Hombourger (PSI)
Guanghua Wang (SINAP)
Jianqiang Wang (SINAP)
Hongjie Xu (SINAP)
Chong Zhou (SINAP)
Yang Zou (SINAP)

Students

Harry Andreades (UCB, Facilitator)
James Kendrick (UCB, Facilitator)
Mohamed Abou Dbai (UW)
Kazi Ahmed (UW)
Amir Ali (UNM)
Manuele Aufiero (UCB)
Pietro Avigni (GT)
Karl Britsch (UW)
Francesco Carotti (UW)
Louis Chapdelaine (UW)
Thomas Chrobak (UW)
Daniel Curtis (MIT)
Tim Flaspoehler (GT)
Ruchi Gakhar (UW)
Andrew Greenop (UCB)
Lakshana Huddar (UCB)
Joel Hughes (UNM)
Chacha Lin (OSU)
Qiuping Lu (OSU)
Lance Maul (ANSTO/UCB)
Samuel McAlpine (MIT)
Arpil Novak (UCB)
Nisarg Patel (UW)
Chris Poresky (UCB)
Floren Rubio (UNM)
Dan Shen (UCB)
Stefano Terlizzi GT
Xin Wang (UCB)
Huali Wu (UW)
Yuyun Zeng (MIT)
Dingkang Zhang (GT)

UCBTH-16-002

April 13-15, 2016

Department of Nuclear Engineering
University of California, Berkeley

This research is being performed using funding received from the U.S. Department of Energy Office of Nuclear Energy's Nuclear Energy University Programs.

Preamble

The University of California, Berkeley; Massachusetts Institute of Technology; University of Wisconsin, Madison; University of New Mexico; Georgia Institute of Technology; The Ohio State University; and Texas A&M University, are collaborating to conduct a series of code-to-code comparison and code validation exercises under two U.S. Department of Energy-sponsored Integrated Research Projects (IRPs) to develop the technical basis to design and license fluoride-salt-cooled, high-temperature reactors (FHRs).

The IRPs hosted a second FHR Code Benchmarking expert workshop April 13-15, 2016, in Berkeley, California, to review code benchmarking needs for FHRs and to obtain advice from experts on best practices for code benchmarking. Experts from Oak Ridge National Laboratory, Idaho National Laboratory, the Shanghai Institute of Applied Physics, and the IRP universities, among others, participated.

This report summarizes results from the Thermal Hydraulics Working Group (THWG) sections of the workshop, and recommends future IRP activities for the THWG.

Executive Summary

Since the original concept of fluoride salt cooled, solid fueled high temperature reactors (FHRs) was first proposed in 2002 [1], substantial progress has been made in understanding the neutronics, thermal hydraulics, and materials issues posed by this technology. These studies have found that FHRs are likely to have high levels of intrinsic safety, enabled by the high volumetric heat capacity and intrinsically low pressure of fluoride salt coolants, and by the very large thermal margins, exceeding 700°C, to fuel damage during transients and accidents.

Given these attributes, in the United States significant effort has been made to develop the scientific and technical basis to design and license FHRs, including work to develop pre-conceptual FHR designs, as illustrated in Fig. P-1, to construct separate effect and integral effect test facilities to validate thermal hydraulics models, and to test FHR structural materials in static corrosion tests both in and out of reactors. In China, rapid parallel progress is underway in the Thorium Molten Salt Reactor (TMSR) program to construct and run salt loops and to design a 10-MWt FHR test reactor, the TMSR-SF1, as well as a 2-MWt, electrically heated TMSR-Simulator.

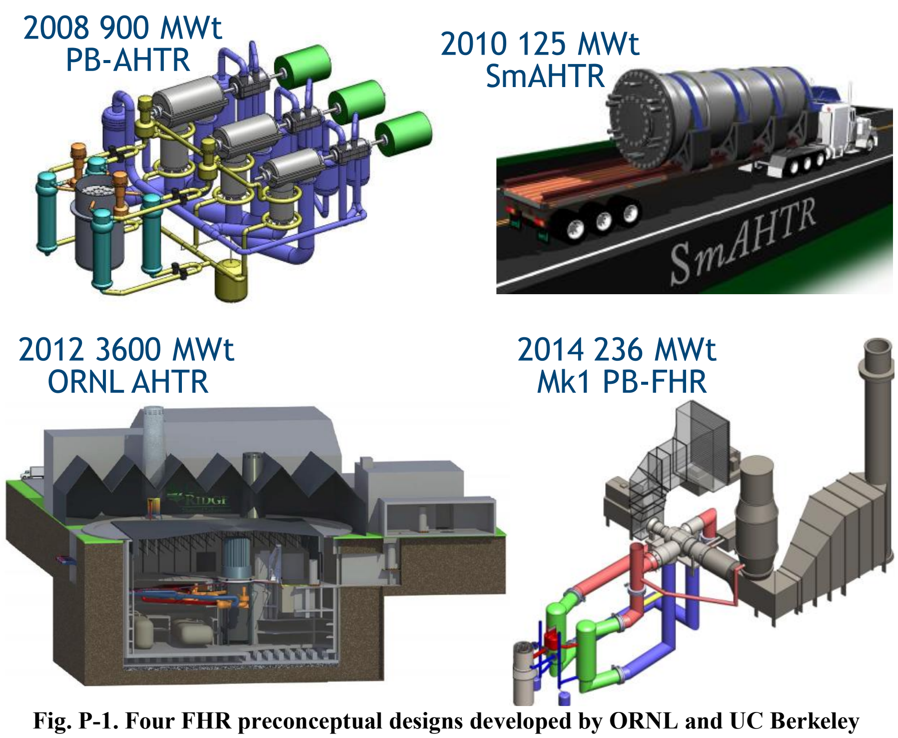

Fig. P-1. Four FHR preconceptual designs developed by ORNL and UC Berkeley

In 2012, the University of California, Berkeley; Massachusetts Institute of Technology; and University of Wisconsin, Madison, conducted a series of expert technical workshops to assess key areas important to the design and licensing of FHRs. These workshops identified major design options and subsystems for FHRs, identified and reviewed key FHR phenomenology, identified key licensing basis events, and recommended a range of general-purpose modeling codes that can be adapted to use for simulation of FHR neutronics, thermal hydraulics, and structural mechanics.

To be used in safety analysis reports for license applications to the U.S. Nuclear Regulatory Commission, simulation codes (referred to as "evaluation models, or EMs") must be validated by comparison with appropriate separate effect and integral system test data, and by benchmarks with other codes, as described in detail in the NRC Regulatory Guide 1.203 [2]. The Guide states,

> "…an assessment should be made regarding the inherent capability of the EM to achieve the desired results relative to the figures of merit derived from the [General Design Criteria]. Some of this assessment is best made during the early phase of code development to minimize the need for later corrective actions. A key feature of the adequacy assessment is the ability of the EM or its component devices to predict appropriate experimental behavior. Once again, the focus should be on the ability to predict key phenomena, as described in the first principle. To a large degree, the calculational devices use collections of models and correlations that are empirical in nature. Therefore, it is important to ensure that they are used within the range of their assessment." (pg. 4)

This report builds upon the descriptions of thermal hydraulic resources within the THWG, and recommends an approach to code benchmarking efforts during the final year of IRP research.

Contents

List of Figures

List of Tables

Acronyms and Abbreviations

AHTR – Advanced High-Temperature Reactor
ANL – Argonne National Laboratory
ANS – American Nuclear Society
ARE – Aircraft Reactor Experiment
AOO – anticipated operational occurrences
ASME – American Society of Mechanical Engineers
ATWS – anticipated transient without scram
BDBE – beyond design basis event
BPV – Boiler and Pressure Vessel (Code)
CFR – U.S. Code of Federal Regulations
CFRC – carbon fiber-reinforced composite
CTF – Component Test Facility
DOE – U.S. Department of Energy
DRACS – Direct Reactor Auxiliary Cooling System
EAB – exclusion area boundary
EDMG –Extensive Damage Mitigation Guidelines
FHR – fluoride-salt-cooled, high-temperature reactor
FHTR – FHR Test Reactor
GDC – NRC General Design Criteria
GT-MHR – Gas-Turbine Modular Helium-Cooled Reactor
H2TS – hierarchical two-tier scaling (analysis)
HTGR – high-temperature gas-cooled reactor
HVAC – heating, ventilation, and air conditioning
IRP – Integrated Research Project
LBE – licensing basis events
LMFBR – Liquid Metal Fast Breeder Reactor
LMR – liquid metal reactor
LOFC – loss of forced circulation
LOHS – loss of heat sink
LS-VHTR – Liquid Salt Very High-Temperature Reactor
LWR – light-water reactor
MSBR – Molten Salt Breeder Reactor
MSR – molten salt reactor
MSRE – Molten Salt Reactor Experiment
NGNP – Next Generation Nuclear Plant
NRC – U.S. Nuclear Regulatory Commission
ORNL – Oak Ridge National Laboratory
PASSC – Plant, Areas, Systems, Subsystems, and Components
PB-AHTR – Pebble Bed Advanced High-Temperature Reactor
PBMR – Pebble Bed Modular Reactor
PCU – power conversion unit
PIRT – Phenomena Identification and Ranking Table
PRA – probabilistic risk assessment

PWR – pressurized-water reactor
SAMG – Severe Accident Management Guidelines
SAR – Safety Analysis Report
SDC – Safety Design Criteria
SFR – sodium-cooled fast reactor
Sm-AHTR – small modular Advanced High-Temperature Reactor
S-PRISM – Super-Power Reactor Innovative Small Module
SS – stainless steel
SSCs – systems, structures, and components
TEDE – total effective dose equivalent
TLRC – Top-Level Regulatory Criteria
TRISO – tristructural-isotropic
UCB – University of California, Berkeley

1 Introduction

Recent studies suggest that fluoride salt cooled high temperature reactors (FHRs), which use solid TRISO fuel, could have exceptional safety characteristics and deliver heat at high average temperatures, in the range from 600°C to 800°C. Noting this, the U.S. Department of Energy has supported two new Integrated Research Projects, with two university teams comprised of MIT, UC Berkeley, University of Wisconsin, and University of New Mexico, along with a second team comprised of Georgia Tech, Ohio State, and Texas A&M, to perform studies to further develop the technical basis to design and license commercially attractive FHRs.

These IRPs are conducting coordinated work to address key technical issues in the areas of FHR thermal hydraulics, neutronics, and materials, chemistry and tritium transport. This white paper describes progress in thermal hydraulics, and summarizes results from the Thermal Hydraulics breakout session of the second FHR Code Benchmarking expert workshop April 13-15, 2016, in Berkeley, California.

1.1 Thermal Hydraulics Working Group – Purpose

The FHR IRP Thermal Hydraulics Working Group (THWG) was formed to develop and participate in code benchmarking exercises, to validate key thermal hydraulics safety codes for use to predict FHR steady state and transient response. The THWG coordinates its activities with the FHR IRP Neutronics Working Group (NWG), including identifying needs for benchmarking problems for coupled thermal hydraulics and neutronics. The THWG has been identifying both separate effect and integral effect tests appropriate for code benchmarking, and coordinating benchmarking calculations.

1.2 Benchmarking Goals

To be used in safety analysis reports for license applications to the U.S. Nuclear Regulatory Commission, simulation codes (referred to as "evaluation models, or EMs") must be validated by comparison with appropriate separate effect and integral system test data, and by benchmarks with other codes, as described in detail in the NRC Regulatory Guide 1.203 [2]. The Guide states,

> "…an assessment should be made regarding the inherent capability of the EM to achieve the desired results relative to the figures of merit derived from the [General Design Criteria]. Some of this assessment is best made during the early phase of code development to minimize the need for later corrective actions. A key feature of the adequacy assessment is the ability of the EM or its component devices to predict appropriate experimental behavior. Once again, the focus should be on the ability to predict key phenomena, as described in the first principle. To a large degree, the calculational devices use collections of models and correlations that are empirical in nature. Therefore, it is important to ensure that they are used within the range of their assessment." (pg. 4)

The goal of the THWG is to lay out and prioritize needs for thermal hydraulics EM assessment for FHRs, and to recommends approaches to code benchmarking efforts.

2 Overview of IRP University Thermal Hydraulic Research

This chapter provides an overview of key FHR thermal hydraulics research activities underway at IRP universities.

2.1 University of California, Berkeley

UC Berkeley has a wide range of thermal hydraulics experimental activities organized to provide key separate effect test and integral effect test data. The majority of these experimental activities use heat transfer oils as simulant fluids for convective heat transfer of the FHR molten salt flibe. These experiments are overviewed briefly here, and more detailed discussion is provided in Chapter 3 (separate effect tests) and Chapter 4 (integral effect tests). Experimental data is used to validate models, as a part of the larger benchmark campaign involving all IRP members as well as outside participants. The coupling of models in thermal hydraulics, neutronics, and structural mechanics for a holistic view of FHR phenomena and response is also a goal for this effort.

Additional students (April Novak and Chris Poresky) were added to this research area and time has been spent for their literature review, training, and research planning. Several undergraduate research assistants have also been trained to work in this research area. The culmination of these additions has been the creation of a, "CIET Team," of seven members (three graduate, four undergraduate) that will be dividing the research tasks and working concurrently through the semester's end. The primary research task for this semester is to improve the RELAP5-3D models of the CIET facility as well as the Mk1 PB-FHR, and to verify and validate these models through experimentation using the CIET facility. Uncertainty quantification will be of particular concern throughout this process. Supporting research tasks are improving the similitude of the CIET facility by changing the physical construction (adding guard heating to limit parasitic heat losses, modifying the heating assembly, etc.), and reassessing the scaling between the CIET facility and the Mk1 PB-FHR through the use of a novel scaling methodology, the Dynamical Systems Scaling (DSS) methodology.

UCB currently has two major separate effect test experimental activities.

The Pebble-Bed Heat Transfer Experiment (PBHTX) is a scaled facility designed to measure heat transfer coefficients within a pebble-bed test section for the conditions applicable to the Pebble-Bed Fluoride-Salt-Cooled High Temperature Reactor (PB-FHR). A simulant oil called Dowtherm A is used as the heat transfer fluid, which matches the Prandtl number of flibe at temperatures lower than the PB-FHR conditions. A dimpled test section 0.0889m long is filled with randomly packed 0.00635m diameter copper pebbles, some of which are instrumented with thermocouples to measure temperature. The inlet and outlet fluid temperatures are also recorded. A Coriolis flowmeter is used to measure the mass flow rate of the oil within the loop. A power supply is used to vary the heater power sinusoidally, and in this way the frequency response of the test section can be measured to a high accuracy. The facility is designed so that the range of Reynolds and Prandtl numbers are matched with the prototypical conditions. The loop has been built using flexible stainless steel piping and tri-clamp fittings. It is built in a modular fashion, implying that the pebble-bed test section could be replaced for future tests. Figure 4.3 shows this test facility currently under construction and preliminary data will be collected starting next month.

The Cartridge Heater Experiment (CHEX) was designed to test similitude between Dowtherm A and fluoride salt for natural convection heat transfer from a vertical cylinder. Experiments were conducted in Dowtherm A and were compared to results from Oak Ridge National Laboratory (ORNL) using flinak. Both laminar, transition and turbulent conditions were investigated. Data collection and data processing is complete, and simulation work is underway to complement the experimental results.

The Compact Integral Effects Test (CIET 1.0) facility is designed to provide data on integral transient thermal hydraulic response of FHRs under forced and natural circulation, particularly startup and shutdown transients, loss of forced cooling (LOFC) and loss of heat sink (LOHS) accident transients, and passive, buoyant shutdown rod insertion during transients. CIET 1.0 has two coupled flow circuits that replicate the primary coolant flow circuit in FHRs, including bypass flow, and the DRACS flow circuit, a natural-circulation-driven loop designed to passively remove decay heat from the FHR core and reject it to the environment through a thermosyphon-cooled heat exchanger (TCHX). Figure 1 shows a photograph of the facility. As an IET, the driving purpose of CIET 1.0 is to provide validation data for evaluation models of FHR thermal hydraulic systems, such as RELAP5-3D, so that the evaluation models may be used to provide a licensing basis for advanced FHR designs. The ability of IETs to perform this work and aid in the process of reactor design licensing was proven by the APEX-AP1000 facility [22].

Figure 1. CIET 1.0 test facility.

2.2 University of New Mexico

The University of New Mexico currently has active experimental research supporting FHR development. This research can be divided into roughly two categories: heat transfer and mass transfer, where in some cases, the research problems are coupled. The heat transfer research is focused on addressing data needs for performance of heat exchangers under the conditions specific to the FHR: low flow rates, moderately high Prandtl number, and conditions where buoyancy effects will be important. Additional information is needed specifically for enhanced heat exchangers (such as twisted tubes), where data in these conditions is not available and it is unclear whether existing correlations will be adequate for design and licensing purposes. More detail on the specifics of the testing is included in the separate effects test experiments section below. The mass transfer research is focused on addressing the challenging level of tritium production in the FHR when utilizing certain primary coolants such as flibe. This research is investigating the use of ultrasonically enhanced inert gas sparging for removing and sequestering tritium produced in the reactor during normal operation.

The major experimental facility that UNM is using to produce heat transfer data is the heat transfer facility shown in Figure 2. The facility is a reduced scale SET experiment designed to reproduce similitude of heat transfer for a range of conditions expected in the FHR heat exchangers (particularly the DHX) using a simulant fluid, Dowtherm A. In addition, the facility is supported under an NEUP to test double-wall twisted-tube heat exchangers which feature an intermediate annulus that can contain a tritium getter (different options are currently under consideration).

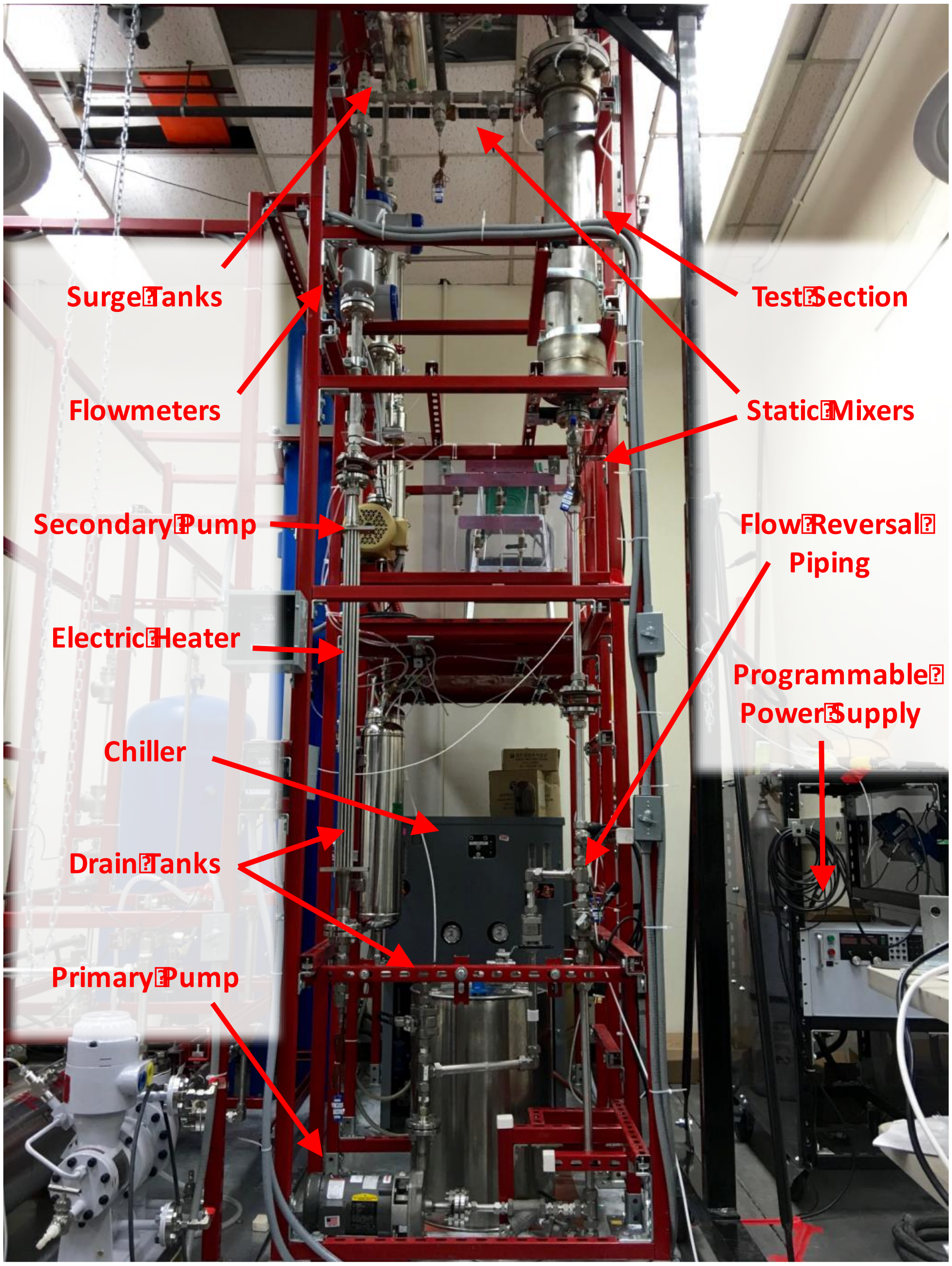

Figure 2. Heat transfer facility at UNM.

2.3 University of Wisconsin, Madison

The University of Wisconsin at Madison has three groups conducting research on thermal hydraulics in the FHR. First, Professor Kumar Sridharan and Professor Mark Anderson are leading Karl Britch to build a materials research FLiBe salt loop that is driven by natural circulation for the Nuclear Materials Group. This salt loop will also be capable of conducting integral effects tests of FHR decay heat removal systems by controlling heat insertion and the buoyant head. While this loop is designed primarily for materials research, it will offer the capability of conducting natural circulation experiments for integral effects tests. A CFD model of the experimental loop has been developed in ANSYS, as part of the experimental design process, and to help with data interpretation.

Secondly, Professor Raluca Scarlat leads the Heat and Mass Transport Group, which has ongoing computational and experimental projects. Mohamed Abou Dbai is conducting scaling analysis, natural circulation stability analysis, and system-modeling of natural circulation loops with multiple branches in COMSOL [3], [4]. Kazi Ahmed is developing system level and component-level models for freezing. A freezing module for system-level modeling is being developed in MOOSE, and will be applied in the system code SAM. This work is in collaboration with Dr. Rui Hu and Dr. Tom Flannagan from Argonne National Lab. SAM is a single phase thermal-hydraulic code written on the MOOSE platform, which branched off from the RELAP7 code development, in order to focus development on problems specific liquid metal reactors, and has no two-phase flow capability. This project will also lead to the first application of system modeling in SAM to FHRs. This tool will enable the modeling of overcooling transients that involve freezing and thawing. This effort is supported by a three-year NEUP grant.

Component-scale modeling and separate-effects experiments are underway, in order to generate closure models for freezing in heat-exchanger tubes: convective heat transport between the solid and the liquid, and friction losses. Kazi Ahmed has developed a CFD model of freezing in a heat exchanger tube in COMSOL. Louis Chapdelaine is conducting a separate effects experiment to study the supercooling effect in the salt, and the freezing behavior as a function of geometry and heat flux; he has also developed a CFD model of the experimental set-up in COMSOL, to aid in experimental design and data analysis. These experiments will be performed with FLiNaK and FLiBe to study the suitability of FLiNaK as a surrogate for FLiBe in freezing experiments; alternative surrogate and simulant fluids will also be studied. The capability of these experimental set-ups to also measure thermophysical properties of the liquid and the solid are being investigated [4].

The Heat and Mass Transport Group is building an optical spectroscopy cell for molten salts, which will be capable of measuring the infrared absorption spectra of salts, including FLiBe salt. It will also be capable of measuring emissivity of surfaces submerged in salt. This work is in collaboration with Professor Mikhail Kats, from the Electrical Engineering Department at the University of Wisconsin Madison. Radiative heat transport will be added to the component-scale CFD models.

2.4 The Ohio State University (IRP Partner)

A low-temperature DRACS test facility (LTDF) and a high-temperature DRACS test facility (HTDF) have been designed and constructed at OSU to study the thermal performance of the natural circulation/convection driven DRACS system during transients. RELAP5/SCDAPSIM/ MOD 4.0 has been selected to perform the system analysis for both DRACS test facilities. Benchmarks of two DRACS transient scenarios carried out in LTDF using RELAP5 have been performed, including a startup scenario and a pump trip scenario. The startup and pump trip scenarios for HTDF have also been simulated by the RELAP5 code. The objective of the present work is to numerically investigate the DRACS thermal performance in terms of its decay heat removal capability and validate the capability of the RELAP5 code for applications to the DRACS system [5]. In addition, fluid properties of FLiNaK and $KF\text{-}ZrF_4$ have therefore been implemented into the RELAP5/SCDAPSIM/ MOD 4.0. [6].

2.4.1 LTDF and HTDF Models in RELAP5

The 1-D models built in the RELAP5 input deck for the LTDF and HTDF, including the nodalization, are shown Figure 3. There are three loops coupled in both LTDF and HTDF and the main components include a simulated core, DHX, NDHX, fluidic diode, and pump. In the LTDF model, the fluids in the primary and secondary loops are water. In the HTDF, the working fluids in the primary and secondary loops are FLiNaK and $KF\text{-}ZrF_4$, respectively. In addition, the heat transfer correlation and friction factor correlation for low Prandtl number fluids are utilized in the HTDF simulation.

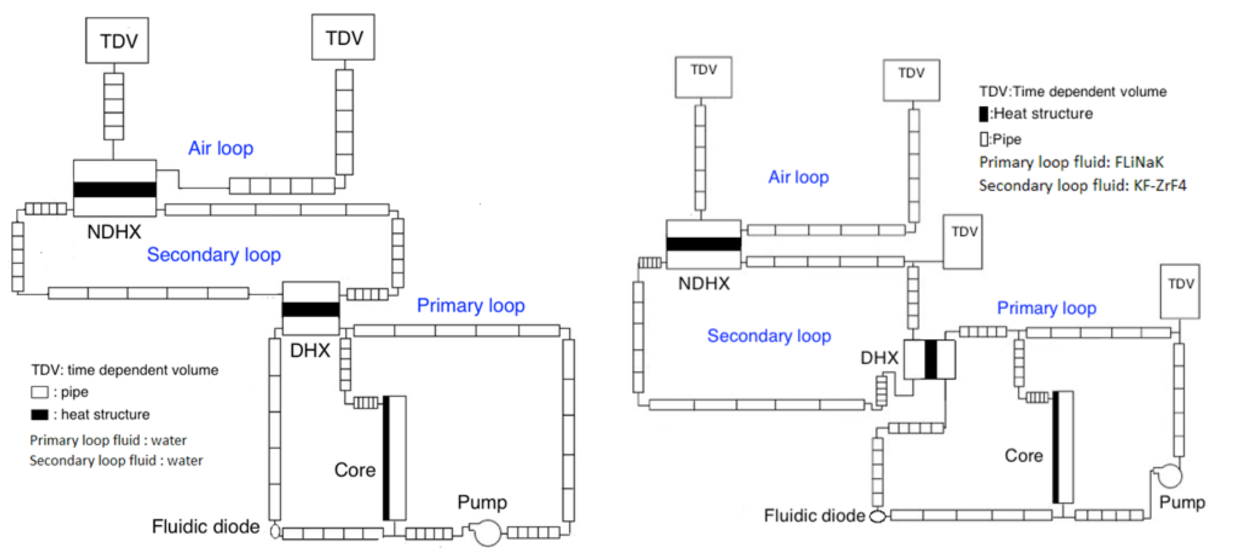

Figure 3. LTDF model (left) and HTDF model (right) in RELA5/SCDAPSIM/MOD 4.0.

2.4.2 LTDF Benchmark Results (Startup Scenario)

The simulation results of the DRACS startup scenario are compared with the experimental data obtained from the LTDF. For the initial condition of the startup scenario, the fluids in all of the three loops are initially stagnant and the fluid temperatures are close to the room temperature. At time zero, a constant power of 2 kW is provided in the simulated core. The temperature profiles of the fluid at the inlet and outlet on the DHX tube side are shown in Figure 4. Natural circulation is gradually established after the core power is activated, resulting in a temperature increase. The simulation results of the fluid mass flow rates in the three loops are compared with the experimental data as well. From Figure 5 the results show that natural circulations are established in the three loops. The air mass flow rate from the RELAP5 simulation is slightly over predicted, which could be due to the measurement uncertainties from the instrumentations. However, the calculation results show similar profiles compared with the experimental data.

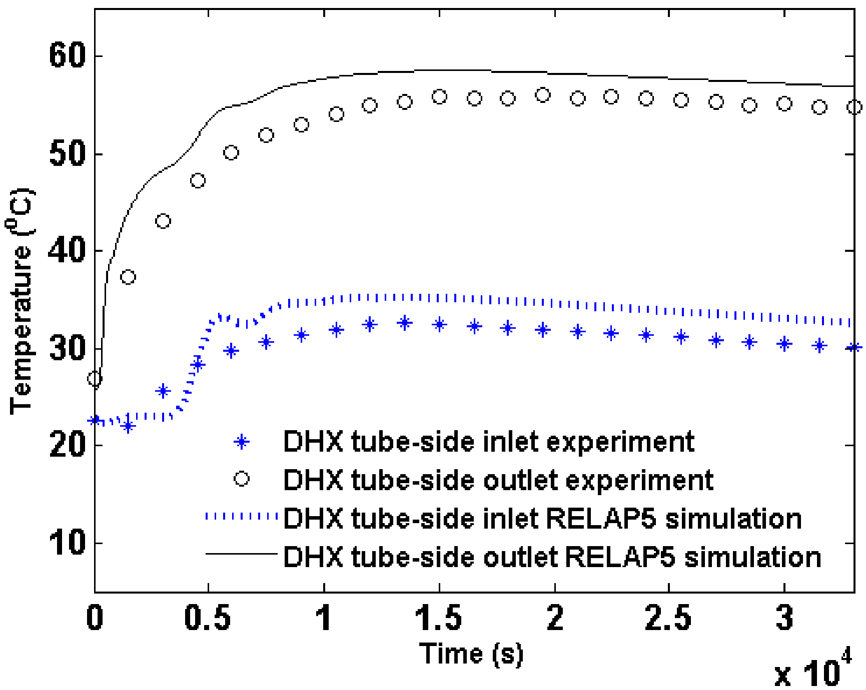

Figure 4. RELAP5 simulation results of the water inlet and outlet temperatures of the DHX tube side compared with experimental data (startup).

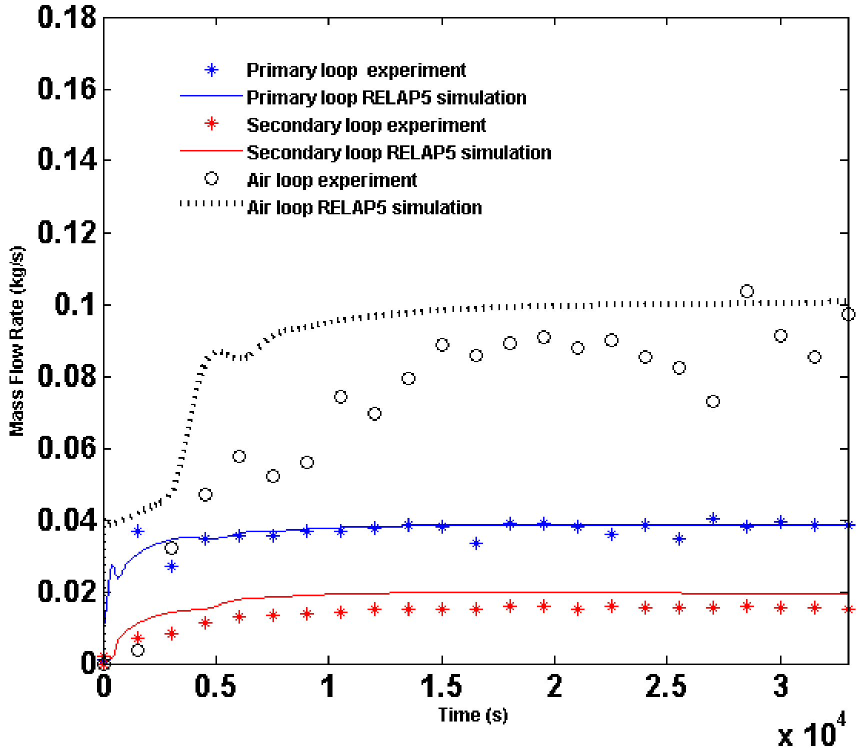

Figure 5. RELAP5 simulations results of the fluid mass flow rates in the three loops of the LTDF compared with experimental data (startup).

2.4.3 LTDF Benchmark Results (Pump Trip Scenario)

Before the transients, the pump is under operation and the whole system reaches steady state. At time zero seconds, the pump is shut down. Figure 6 shows the benchmark results of the fluid temperature profiles in the secondary loops. After the start of the transients, the temperatures of the hot leg and cold leg in the secondary are not changing significantly, since the power provided from the core is not changed after pump is turned off.

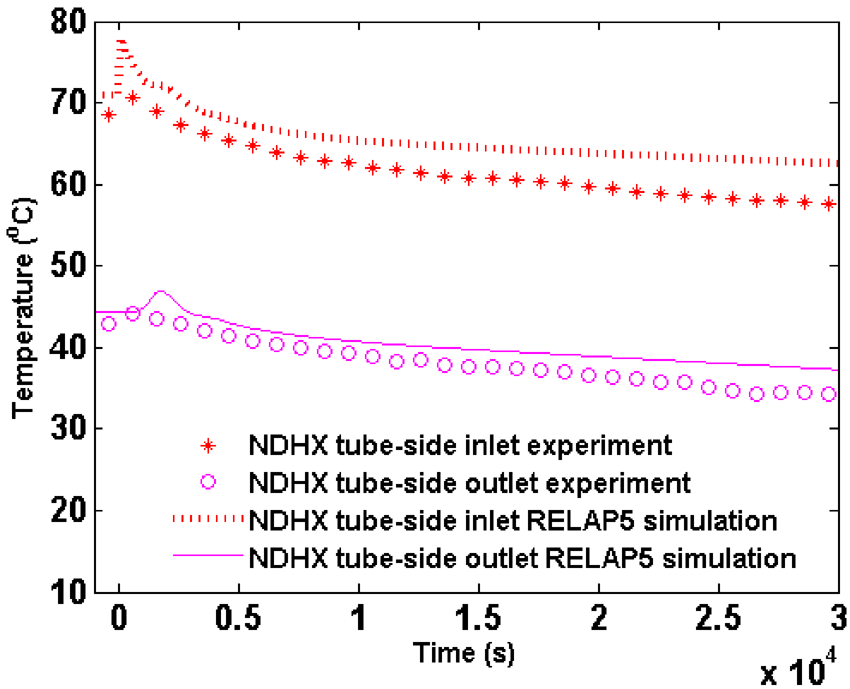

Figure 6. RELAP5 simulations results of the water inlet and outlet temperatures of the NDHX tube side in the LTDF compared with experimental data (pump trip).

2.4.4 HTDF RELAP5 Simulation Results

The experimental data of HTDF is not available at the time this report was written, therefore, only simulation results of the startup and pump trip scenarios are included. Figure 7 shows the temperature profiles in HTDF in the startup scenario. It should be noted that enough temperature margin in the secondary loop cold leg temperature from the freezing point should be provided during the startup transient test [9].

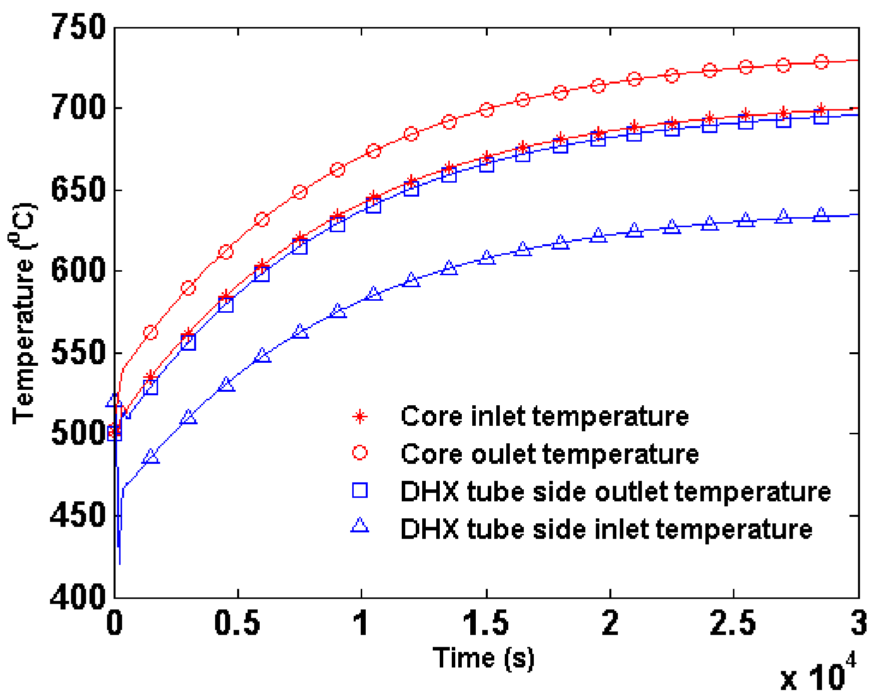

Figure 7. RELAP5 simulation results of the hot leg and cold leg temperatures of the primary and secondary loops in the HTDF (startup).

In pump trip scenario simulation, the mass flow rates of the three loops in the HTDF are shown in Figure 8 (left). After the pump is tripped, the primary flow reverses since it loses the driving force provided by the pump and the buoyancy force and hence the natural circulation in the primary loop starts to develop. In the pump trip scenario, there is no need to worry about the salt freezing because the salt temperatures are above 600°C based on the RELAP5 simulation as shown in Figure 8(right).

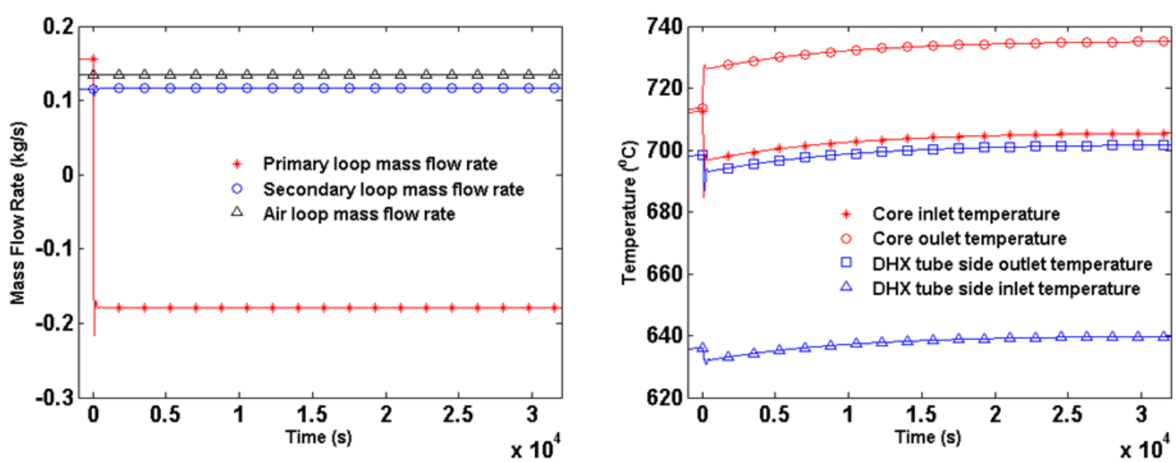

Figure 8. RELAP5 simulation results of the mass flow rates (left) and temperature profiles (right) in the HTDF (pump trip).

3 Separate Effects Test Research Program

Separate effect tests provide key data to validate physics models and constitutive closure relationships used in thermal hydraulics safety models. This chapter reviews SETs being developed and used in the FHR IRPs.

3.1 Purpose of Separate Effects Tests

Separate effect test facilities are one type of experimental facility used to validate thermal hydraulics models and to test FHR components.

To be used in safety analysis reports for license applications to the U.S. Nuclear Regulatory Commission, simulation codes (referred to as "evaluation models, or EMs") must be validated by comparison with appropriate separate effect and integral system test data, and by benchmarks with other codes, as described in detail in the NRC Regulatory Guide 1.203. The Guide states, "…an assessment should be made regarding the inherent capability of the EM to achieve the desired results relative to the figures of merit derived from the [General Design Criteria]. Some of this assessment is best made during the early phase of code development to minimize the need for later corrective actions. A key feature of the adequacy assessment is the ability of the EM or its component devices to predict appropriate experimental behavior. Once again, the focus should be on the ability to predict key phenomena, as described in the first principle. To a large degree, the calculational devices use collections of models and correlations that are empirical in nature. Therefore, it is important to ensure that they are used within the range of their assessment." (pg. 4)

The purposes of separate effects tests are

- Exploration of phenomena
- Component-level testing
- Basis for code validation
- Closure models for system level codes

Because FHRs have multiple phenomena which are either not fully understood or have not been demonstrated, we can use separate effects tests to isolate these phenomena so that the resulting information can be incorporated into integral effects test facilities.

In addition to facilitating the study of isolated phenomena, separate effects tests can be used to study specific system components in order to define their performance for a variety of configurations and conditions that may complement the integral effects test program.

Similarly, the data from these tests can be used in verification, validation, and uncertainty quantification (VVUQ) efforts for simulation codes which are being used to represent isolated phenomena.

Finally, experimental facilities which allow determination of system characteristics for specific components or phenomena can be used to provide information necessary to complete closure models for system level codes such as friction and form loss factors.

3.2 University Separate Effects Test Experiments

There are many phenomena important to FHRs that would benefit from separate effects test experiments. One property that will need to be determined and benchmarked will be the thermal expansion coefficient of both flibe and structural materials. Another set of phenomena that will be important to understand is phase change behavior in simulant fluids such as freezing. While Dowtherm A may provide useful results for heat transfer, the information may have limited usefulness in thermal-hydraulic regimes where two-phase phenomena play a role.

Radiative heat transfer in flibe will also need to be studied using separate effects tests. Current designs have considered flibe to be “transparent” but this is only true for a pure, clean salt. The effect of radiative heat transfer will need to be incorporated in design decisions. Thermal radiation is very different for flinak versus flibe and its assessment may allow applicability of existing models to systems using flibe. This may also be a significant distortion between prototypes and scaled models using Dowtherm A.

Leak behavior will also be important to FHR design and may be suitable for separate effect testing. The TMSR program has some research efforts in this area which have shown that insulation makes it difficult to detect leaks early on. Furthermore, beryllium has proven to be a significant concern when leaking due to the danger coming from aerosols and airborne particulates (beryllium oxides and metallic beryllium in the air).

Because a large amount of the experimental work on FHR thermal-hydraulics is utilizing simulant fluids at a reduced scale, future separate effects tests should focus on validating this data. In order to use the data in design and licensing efforts, the appropriateness of the use of simulant fluids in benchmarking must be evaluated. A related concern is the large uncertainty associated with fluoride salt properties that have also been measured in small applicable temperature ranges. We must reduce the uncertainties in property measurements for flibe, as well as other fluoride salts such as flinak, and take measurements for wider temperature ranges.

Heat exchangers may also require benchmarking because it is difficult to prove that small scale heat exchangers can accurately mimic the local effects of larger ones. Other component-related separate effects test include salt pump testing and fluidic diode testing.

Due to the size and variation of candidate separate effect tests, we should conduct PIRT or PIRT-like activities to determine the array of separate effects tests needed for phenomena not covered in integral effects tests. Information from Ohio State University’s recent PIRT workshop may be useful and informative in this pursuit.

A key point that must be stressed throughout future separate effects testing work is that we must ensure complete and appropriate benchmark selection in order to avoid future delays.

3.2.1 University of California, Berkeley

UCB is currently using the Pebble-Bed Heat Transfer Experiment (PBHTX) to measure the heat transfer coefficient between pebble fuel elements and flibe by using copper pebbles and a simulant oil. The heat transfer coefficient is being measured in a pebble bed test section as a function of position and time for ranges of Prandtl and Reynolds numbers. The experiment currently employs a food-grade mineral oil called Drakesol that is similar to Dowtherm A but easier to work with.

While the primary goal of PBHTX is to determine pebble-coolant heat transfer, the experimental data it generates can also be used to support FHR scaling analysis. Data collected from the experiment could possibly be used to validate similitude of heat transfer oils and fluoride salts.

An additional suggestion was made during the workshop to plot the heat transfer coefficient against the Buoyancy number because buoyancy may be affecting the flow characteristics. An example of this phenomenon is that downward flow has a higher heat transfer coefficient for gases.

Future separate effects tests at UCB could focus on the need to demonstrate similitude between fluoride salts and Dowtherm A for natural convection heat transfer. One experiment might compare Nusselt numbers for matched Prandtl and Grashof conditions by immersing a cartridge heater in flinak and Dowtherm A. The data from such an experiment can be contrasted with Nusselt numbers predicted using correlations for natural convection heat transfer from a vertical flat plate.

3.2.2 University of New Mexico

The two categories of heat exchangers, single wall and double wall, which UNM will be testing in its heat transfer facility are shown in Figure 9 and Figure 10. The single wall tests will be specifically investigating bi-directional heat transfer enhancement in conditions phenomenologically similar to those of the FHR. Low flow rates in the laminar and transitional regimes will be tested using forced circulation in upward and downward flow directions. Natural circulation will also be testing in the downward flow direction. Because the plain tube and twisted tube variants are both manufactured from the same supplier with this testing purpose in mind, the experiment should provide an apples-to-apples comparison of heat transfer and pressure drop performance for the same flow rate and Prandtl number ranges between plain tubes and twisted tubes. This data will be used to test the adequacy of correlations in the literature (for example, see [14]) for use in natural circulation and Prandtl numbers in the 10-15 range. In the most likely case, the Reynolds dependency term in forced convection heat transfer correlations will be replaced with a Grashof dependency for natural circulation flow.

Figure 9. Twisted versus plain tube heat exchangers provided to UNM, masked for clarity (photo credit: Hipex).

Figure 10. Twisted outer/plain inner versus plain outer/plain inner tube heat exchangers provided to UNM.

The double-wall tests will be investigating heat transfer performance of a double-wall twisted-tube heat exchanger concept for mitigating tritium migration through the salt-to-gas heat exchangers in the FHR, simulated by the heat exchangers in Figure 10. In particular, UNM is funded through a DOE NEUP to experimentally explore the use of this concept to couple FHRs to supercritical-CO_2 (S-CO_2) advanced power conversion cycles. The proposed advantages of the concept include the use of twisted outer tubes on the shell-side for heat transfer enhancement in the salt, double-wall design with intermediate tritium getter, and circular inner tube to help accommodate the large pressure differential between the salt and S-CO_2. Several materials are under consideration for use in the intermediate annulus between the tubes. Liquids, gases, and even powders are available as potential tritium getters/barriers and heat transfer mediums. It is also possible to maintain the annulus at an intermediate pressure between the salt and S-CO_2, which may also help provide accommodation for the large pressure differential. UNM will be working with Sandia National Laboratories (SNL) to perform thermal-hydraulic testing on the heat exchangers already provided to UNM and on revised test sections informed by the results of these preliminary experiments.

The heat transfer facility component layout is shown in Figure 11. The facility is composed mainly of two loops: a primary loop and a secondary loop. The primary loop flows water or Dowtherm A through the shell side of the test section (heat exchanger) by natural circulation or by bi-directional forced circulation by means of flow reversal piping and valves located near the primary pump. The secondary loop flows water or Dowtherm A through the tube side of the test section (heat exchanger) by means of the secondary pump. Heat is provided to the primary loop through an electric heater, flows to the secondary loop through the test section, and leaves the secondary loop through the secondary heat exchanger to a chilled water circuit.

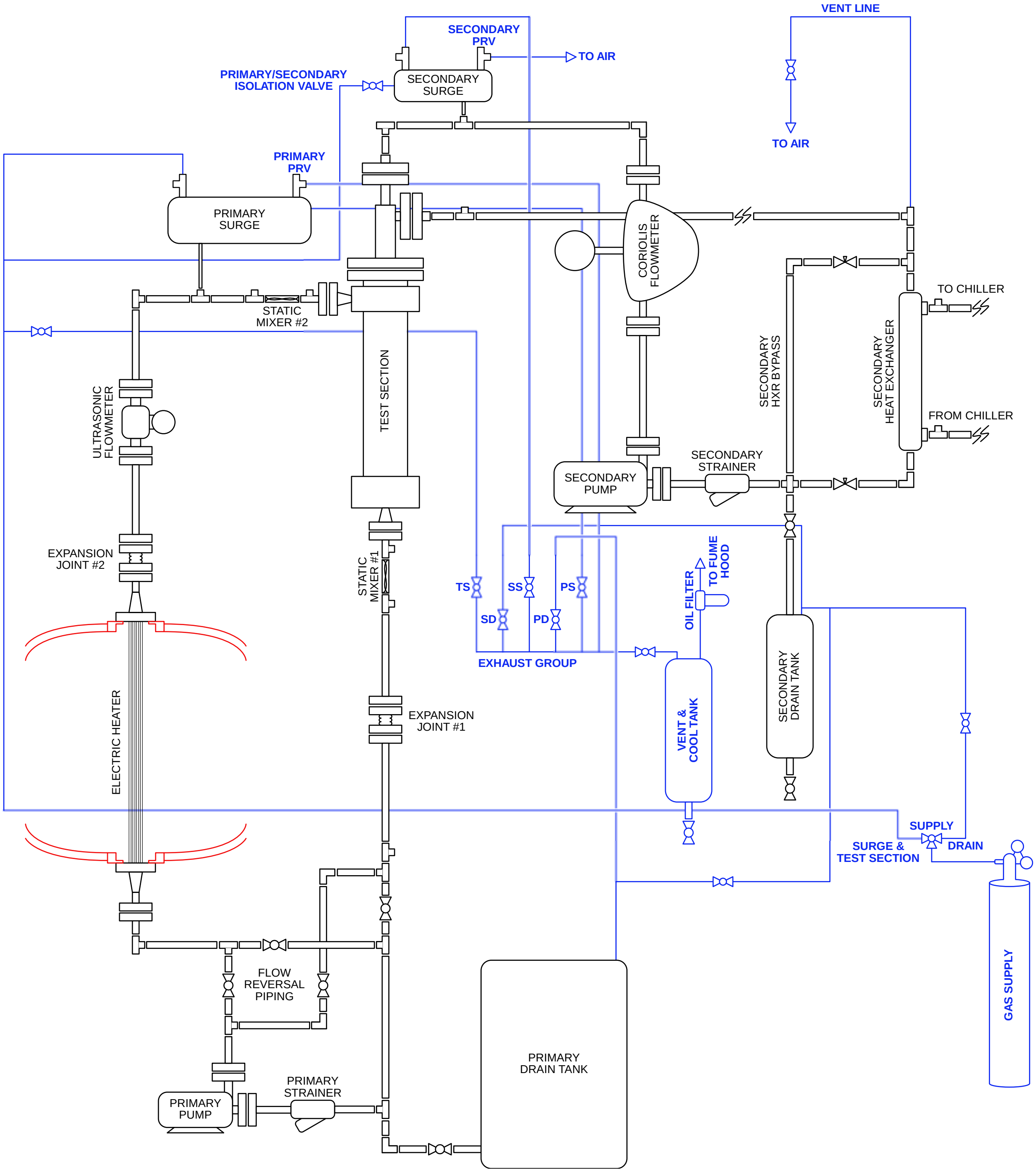

Figure 11. Schematic representation of the heat transfer facility at UNM. The facility is composed of a primary loop, a secondary loop, and a chiller circuit.

Average temperature in the primary loop is controlled by a software PID controller implemented in LabVIEW communicating with a programmable DC power supply. The power supply provides current used for Joule heating in the electric heater. Temperature in the secondary loop can be controlled by adjusting the secondary flow rate, by adjusting the bypass flow fraction through the secondary heat exchanger, and by adjusting the temperature set point on the chilled water supply.

A cover gas system is also installed which utilizes a shared compressed gas supply (e.g. compressed air or nitrogen) to perform initial loop fill, level control, pressure control, and venting functions in the facility. Pressure relief valves are located on both primary and secondary loops for safety, and all vent points will be ultimately routed through a vent and cool tank, which allows liquid collection and cooling of the vapor before routing the fumes to a nearby fume hood.

Data acquisition is performed with a National Instruments software and hardware system. The measurements layout for the facility is shown in Figure 12. The major measurement categories are flow, pressure, and temperature. Flow rates are measured in the primary loop and secondary loop and reported to the data acquisition system via 4-20 mA signals. The primary flowmeter is a Krohne ultrasonic transit time meter, which can measure bi-directional flow and has no obstructions inside the meter (leading to low pressure drop), which is an advantage for natural circulation systems. The secondary flowmeter is a Krohne Coriolis meter, which has better accuracy than the ultrasonic meter, but a higher pressure drop. Flow rate in the chiller circuit is measured via a simple rotameter. Pressure transducers are located in the primary and secondary surge tanks to monitor cover gas pressure.

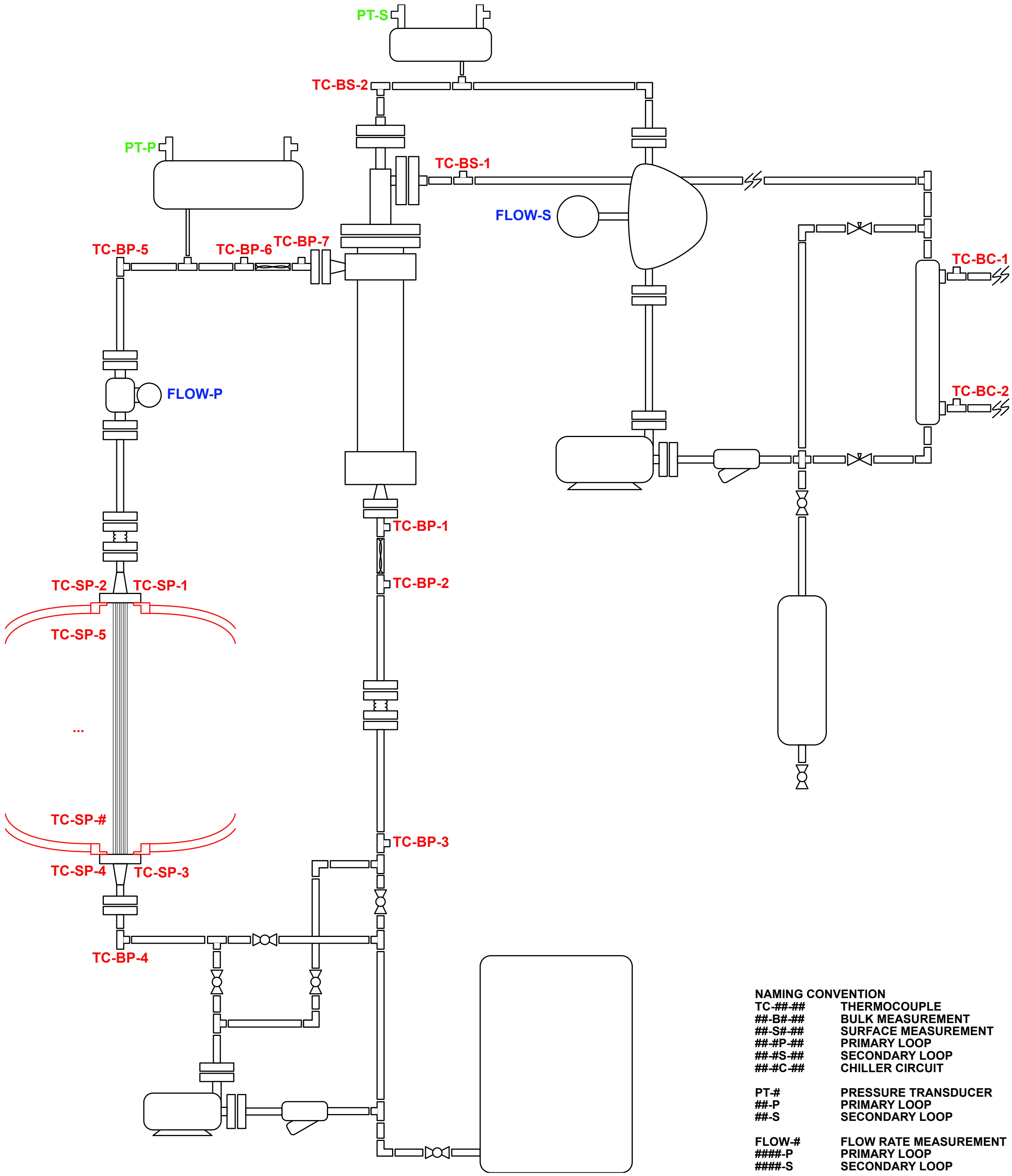

Figure 12. Schematic showing the location of measurements for the heat transfer facility.

Scattered about the loops are a variety of temperature measurements. The primary loop has seven bulk temperature measurements, including two at the entrance and two at the exit of the test section, each pair separated by its own static mixer so that accurate bulk temperature measurements around the heat exchanger can be made even in laminar flow. The secondary loop includes two bulk temperature measurements at the inlet and outlet of the test section. The final two bulk measurements are at the inlet and outlet of the secondary heat exchanger on the chilled water side. Surface thermocouples are located on the electric heater to monitor tube surface temperatures and potential hot spots on the lugs.

Future plans for additional measurements include pressure drop along the length of the heat exchanger. Two sets of five ports distributed circumferentially are located on the test section shell near the upper part of the bundle and near the lower part for the purpose of measuring pressure drop. In addition, several extra ports have been included at the top of the test section shell which can provide through-walls for a fiber-optic-based or other temperature measurements.

In addition to the heat transfer facility, UNM also has a hydrodynamics test loop that has historically been used to do prototyping for a directional heat exchanger concept. The conceptual design is shown in Figure 13. Because the FHR utilizes a fluidic diode to minimize parasitic heat losses in the DRACS during normal operation by limiting bypass flow through the primary DHX branch, a directional heat exchanger concept was developed to explore potential synergies by incorporating fluidic diode design features of different kinds into the heat exchanger itself. The experiment measured flow rates and pressure drop while visualizing flow through the use of dye. Heat transfer performance and thermal diodicity was inferred from the pressure drop data using theory developed with the experiment [15]. The design showed promise and indicated some potential changes might be desirable. A heat transfer test section incorporating these design changes will be tested in the heat transfer facility in the future.

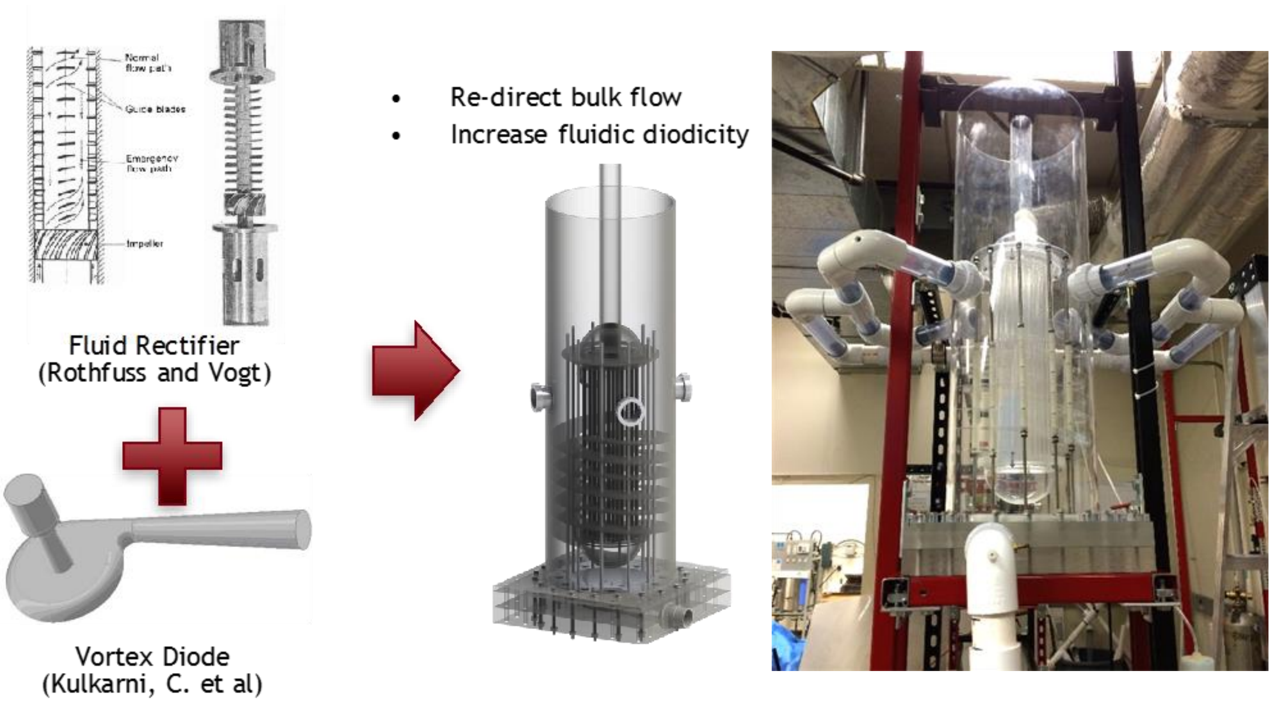

Figure 13. Design concept for a directional heat exchanger (left) and the hydrodynamic test section investigated at UNM (right); more information can be found in [12].

3.2.3 University of Wisconsin, Madison

The Static Freezing Experiment (SFX) at the University of Wisconsin is a first generation experiment to study salt freezing. Its goals are:

1. To investigate supercooling in FLiBe and FLiNaK.
2. To investigate freezing regimes in the heat flux range of 4 to 40 kW/m2.
3. To explore instrumentation options for measurement of freezing front propagation and temperature profile.
4. To crudely measure thermophysical properties close to the melting point.
5. To provide an initial validation dataset for the prediction of freezing front propagation by CFD modeling.

Table 1. Static freezing experiment limiting parameters.

Parameter	Low Limit	High Limit
Sample Volume	50 mL	250 mL
Sample Mass	100 g	500 g
Sample Diameter	46 mm	78 mm
Initial Sample Temperature	470 Celsius	500 Celsius
Cooling Bath Temperature	250 Celsius	450 Celsius
Heat Flux	4 kW/m^2	40 kW/m^2
Grashof Number	1.11×10^6	6.75×10^7

Both FLiBe and FLiNaK will be used as salt samples to be tested. Preliminary data has shown tens of degrees supercooling in FLiBe, and less than five degrees of supercooling in FLiNaK.

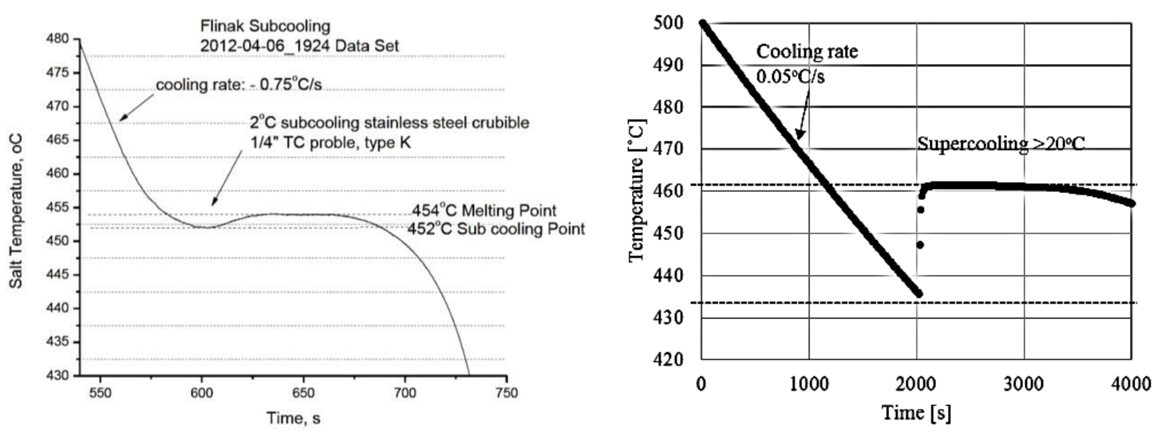

Figure 14. Data observed during cooling of a static sample of FLiNaK upon exposure to a 20°C ambient temperature in a stainless steel crucible (left); data observed during FLiBe handling operations at UW-Madison (right) [3].

A round-bottom flask containing isothermal liquid FLiBe is inserted in a well-stirred liquid bath that is at a temperature below the melting point of FLiBe. A round-bottom flask was selected, because the almost-spherical geometry of the sample makes this a relatively simple system to model. A well-stirred cold bath ensures that the dominant resistance to heat transport is in the sample flask, not on the exterior surface of the sample flask. The temperature of the cold bath is maintained constant, thermal insulation and trace heating with PID control to control its heating power.

The sample flask is instrumented with an array of thermocouples to monitor the evolution of the freezing transient, as shown in Figure 15. Several methods for imaging of the freezing front propagation will be investigated: optical, ultrasound, x-ray.

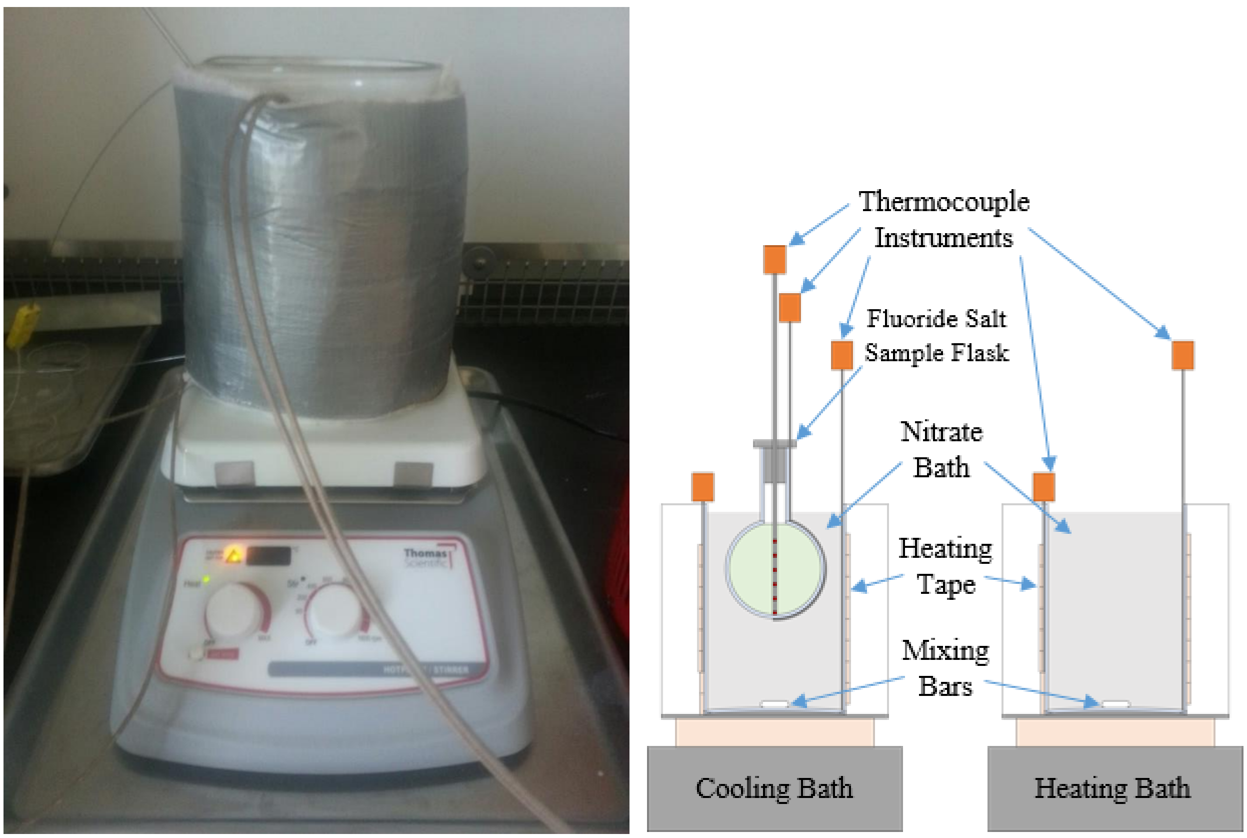

Figure 15. Static freezing experiment nitrate salt bath and hot plate/stir plate (right); static freezing experiment setup, sample flask diameter of 66 mm shown (left).

Currently, Static Freezing Experiment and pipe-flow freezing COMSOL models exist which simulate frozen layer emergence and growth, but do not yet account for supercooling.

The pipe freezing model can be used with a variety of conditions, to help understand the nature of overcooling in pipe geometries. Sample results based on TCHX geometry are shown in Figure 16. The coolant is initially set to a temperature just above freezing, then heat removal during the transient causes the growth of a frozen layer. The plots show radial position in the pipe on the x-axis, with the zero at the center of the pipe. Note that over the course of the transient, a region of zero velocity emerges from the pipe wall and continues to expand. The nozzle-like geometry created by the frozen layer accelerates the fluid in the center, reducing its residence time. The solid layer begins to function as an insulating boundary since a large temperature gradient between the liquid and the pipe surface develops across the frozen layer.

The shortcomings of this model exist in the limitations on boundary conditions. Scenarios like fixed inlet velocity will not exist in a natural circulation decay heat removal system. The development of a frozen layer will increase friction loss, which counteracts the buoyant driving force. However, it will also reduce heat transfer out of the pipe and insulate the liquid center. To truly understand how these coupled effects determine the behavior of a natural circulation system, a system thermal hydraulics code must be used. The System Analysis Module (SAM) at Argonne National Laboratory has been selected as the code of choice for implementation of a freeze-capable pipe, which could be placed in a natural circulation loop, then used to study overcooling transients. The pipe freezing model, and future experiments, can provide the data needed to develop this capability in SAM. In 1D, SAM will need to account for frozen layer thickness which results in an effective reduction in pipe hydraulic diameter and flow area, and alters the overall heat transfer coefficient with the addition of an extra boundary layer.

Thinking outside the pipe, there are some alternatives to the current experiments which may simplify the quest to understand freezing, and also alternatives to cooling system design which may increase system resistance to overcooling. Freezing hot salt on a cold object inserted into the sample might be easy to perform experimentally, as well as model in COMSOL. Flipping the problem on its head, it is also worth considering heat exchangers with salt flow in the shell side over the heat rejection fluid. If freezing occurs, there is still significant area for bypass, so the effect on friction loss is less dramatic. This might actually be the best option to avoid total freeze shut. TCHX could be redesigned as a shell-in-tube heat exchanger with salt on the shell, and with double-walled tubes to ensure radiative heat transfer is still dominant, and mitigate the likelihood of freezing.

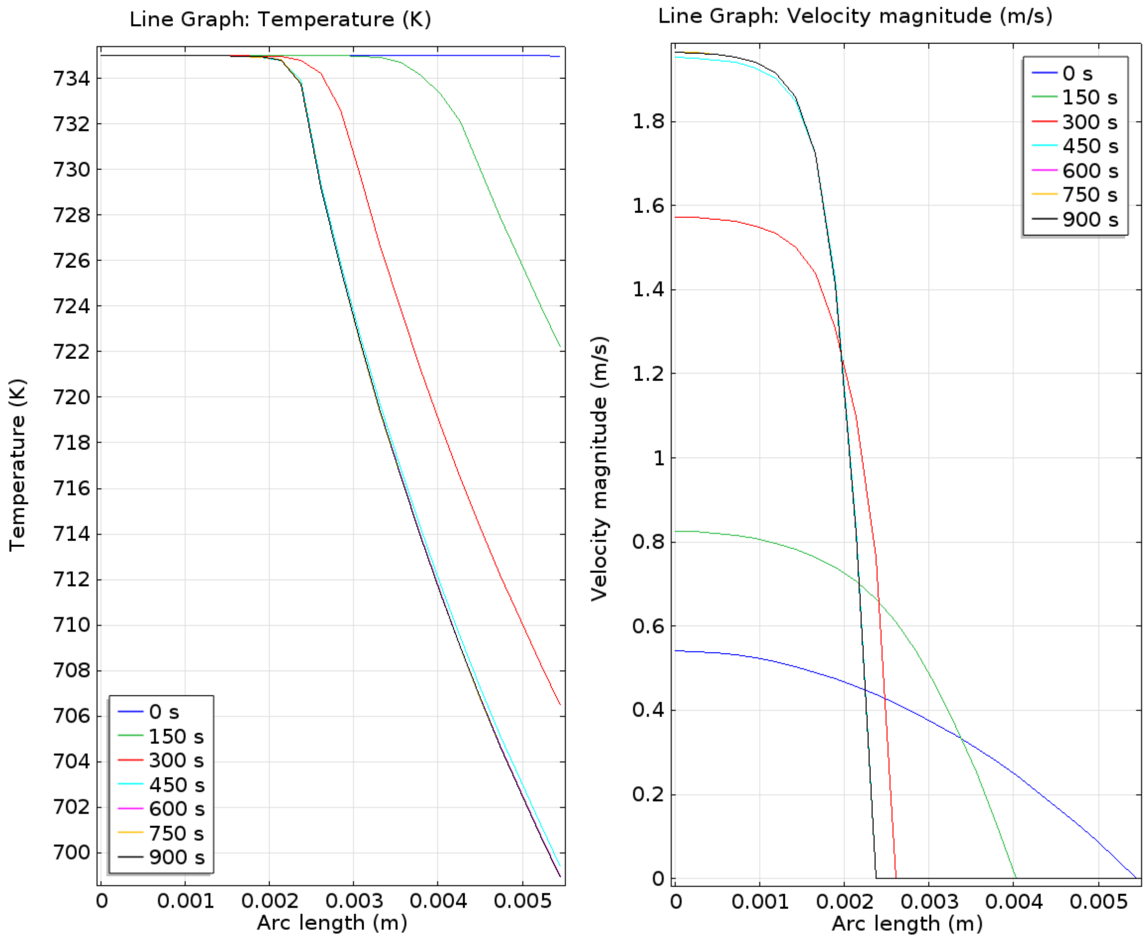

Figure 16. Pipe freezing model cutaway showing freeze front propagation.

Freezing simulation studies are being conducted for pipe freezing and the Static Freezing Experiment. The output of the pipe freezing model is shown Figure 16 and Figure 17, and the output of the Static Freezing model is shown in Figure 18.

The Static Freezing Experiment will serve as the precursor to this experiment by quantifying thermophysical properties of fluoride salts near the freezing temperature, quantifying supercooling in fluoride salts, and verifying the heat transfer model in the absence of salt flow.

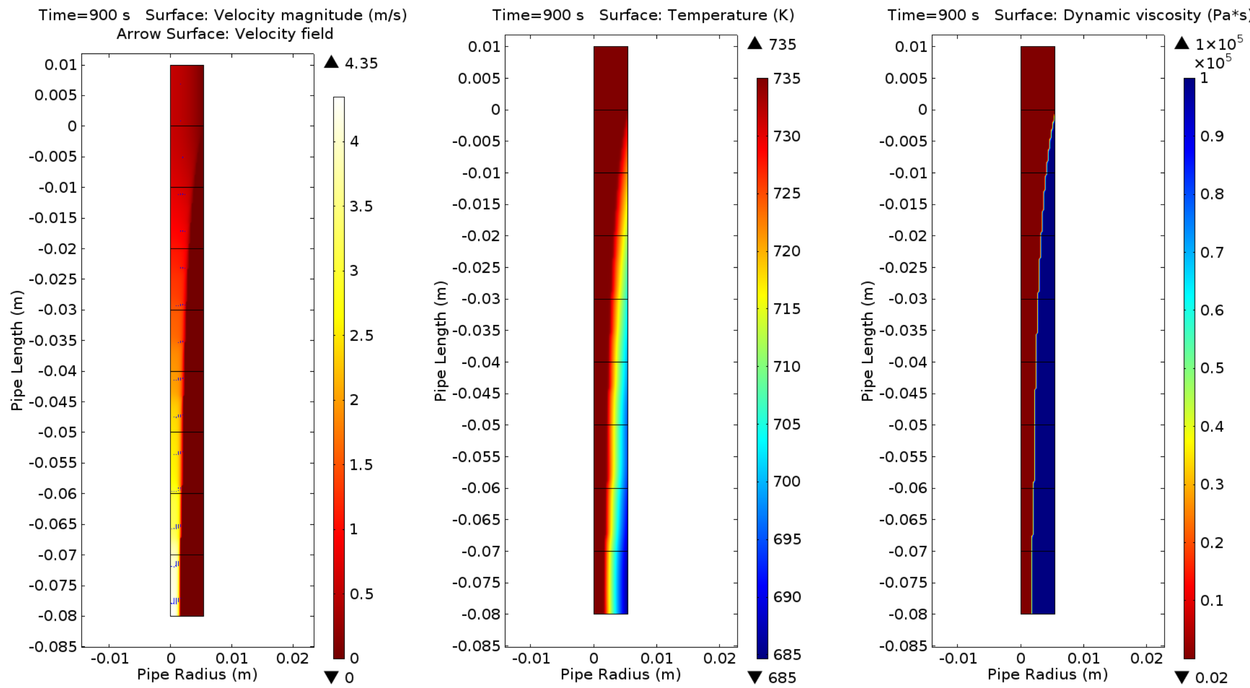

Figure 17. Pipe freezing model results after freezing front fully develops.

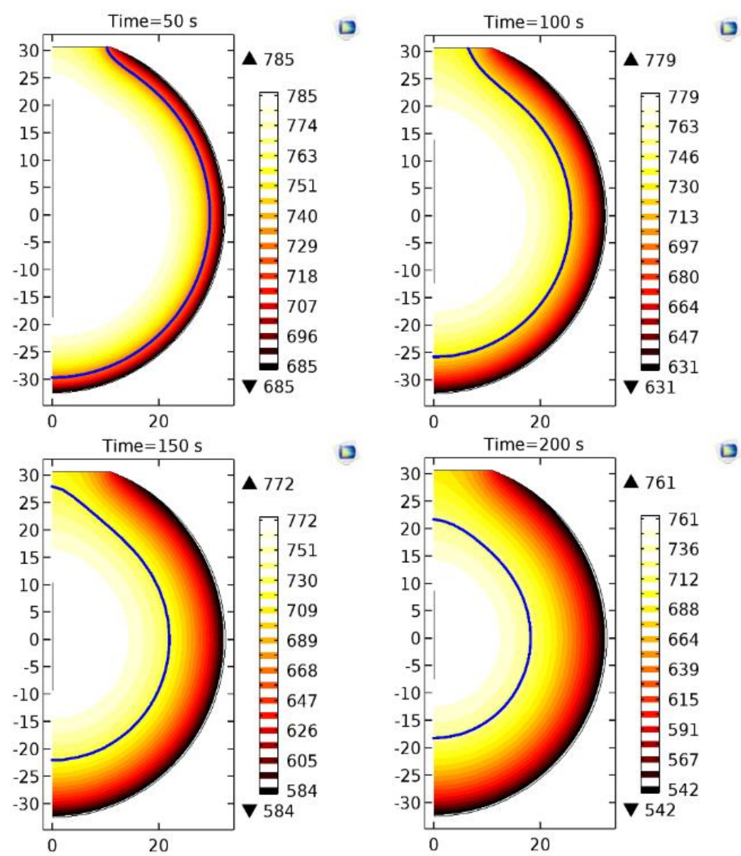

Figure 18. Static freezing model results showing freeze front propagating as the blue line (x- and y-axis are given in mm).

Results from this experiment can also be used to determine whether FLiNaK and FLiBe freezing behavior can be scaled together. Additionally, it appears that Dowtherm A and FLiBe have a similar degree of supercooling in non-dimensional space. Understanding ways to test different materials for supercooling will be invaluable to understand importance of supercooling in FHR coolants. If supercooling is proven to be significant in FHR systems, its stochastic behavior creates a significant modeling challenge. As a result, it is important to determine the significance of supercooling in fluoride salt freezing in the FHR systems in order to model it successfully.

This study will culminate in the development of the freezing module of SAM. Finally, it would be highly beneficial to explore the ability of a salt system to freeze-heal pipes, as well as the effect of salt leakage on systems such as the trace heating and insulation.

3.2.4 The Ohio State University

The primary SET studied at OSU is the vortex diode. The vortex diode effectively blocks flow in one direction and allows flow in the opposite direction. The vortex diode will be critical for the DRACS system in the FHR to function effectively during accident scenarios but to draw minimal power from the reactor during all other conditions.

Previously, a vortex diode was designed following a parametric CFD study. To validate the design, the fabricated vortex diode was first tested with water to examine its pressure drop characteristics in both forward and reverse flow directions. The test results are shown in Figure 19 and Figure 20, along with the predictions from the correlations earlier developed in the parametric CFD study. Overall, the agreement is good, especially considering the geometric difference between the fabricated vortex diode and simulated one, as well as the difference in the fluids. The test results validate our previous CFD studies of the vortex diode to some extent, and add to our confidence in the correct functioning of the vortex diode for application to the HTDF.

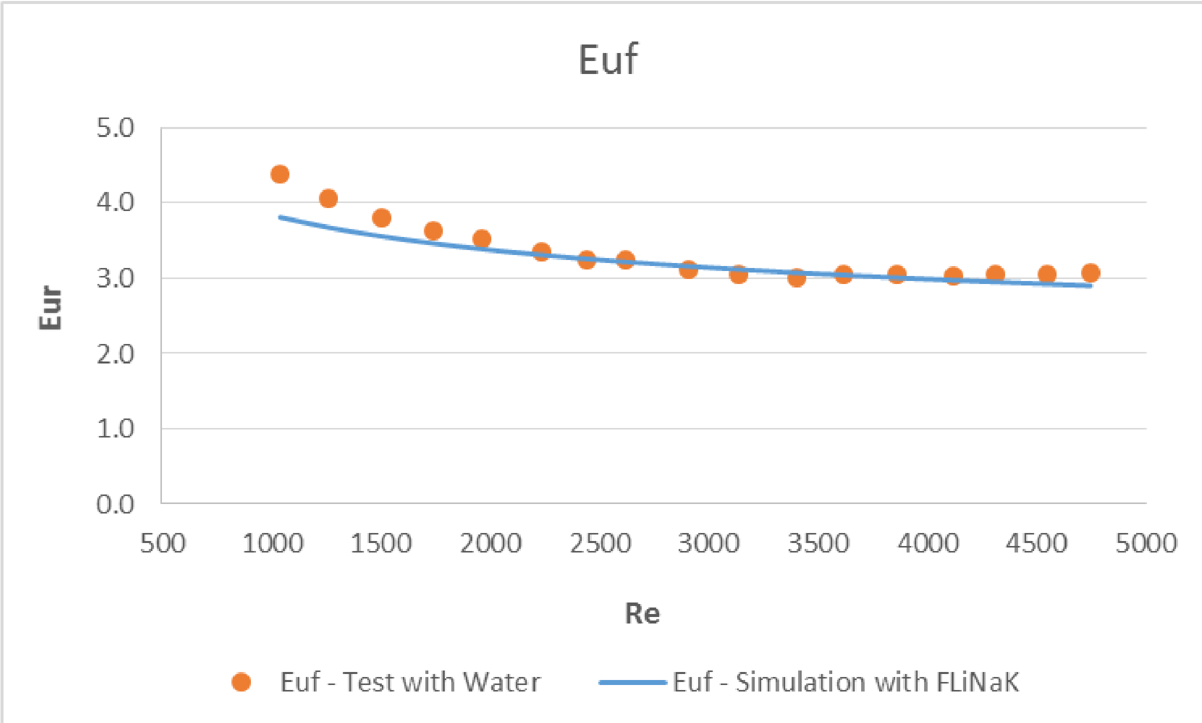

Figure 19. Measured and simulated Euler number for the forward flow direction.

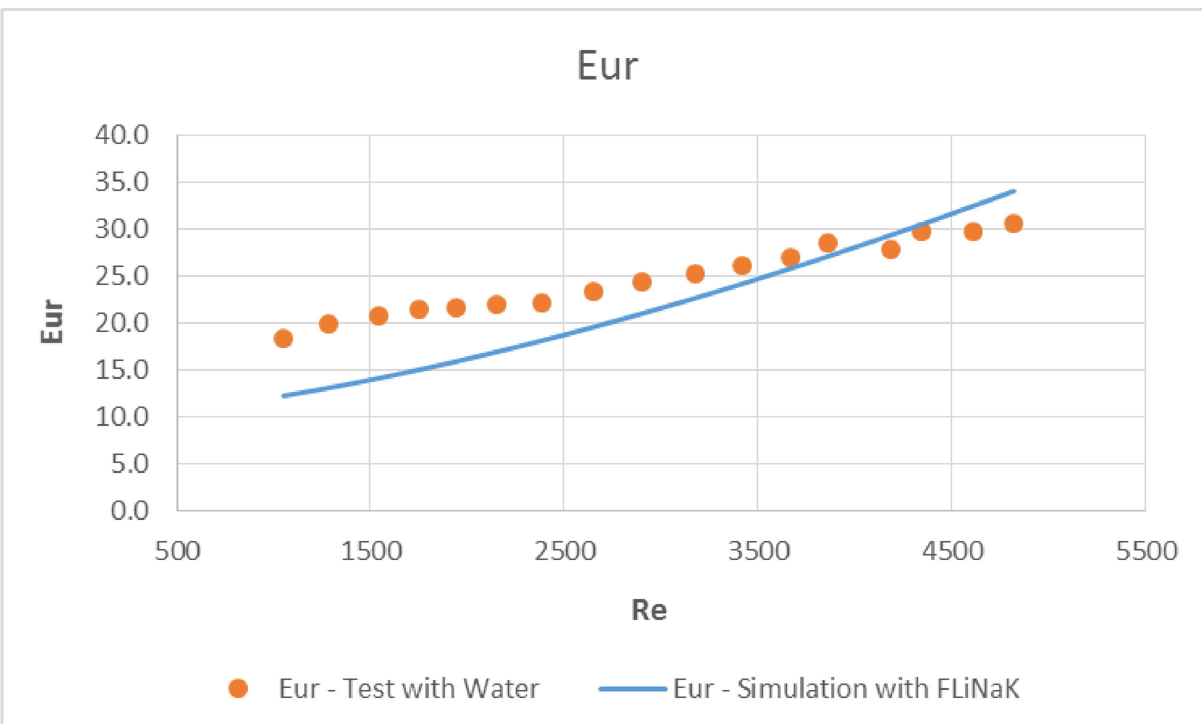

Figure 20. Measured and simulated Euler number for the reverse flow direction.

3.3 Example Separate Effects Test Benchmark

Two candidate benchmarking exercises were proposed in the first IRP workshop [16]. The first, candidate exercise 1 (CE1), proposed testing simple natural circulation at steady-state. UNM's heat transfer facility is well set-up to perform this exercise, as it is designed to investigate heat transfer performance of heat exchangers during steady-state natural circulation. The second proposed exercise, CE2 was to perform a transient response following protected and unprotected LOFCs. UNM's facility was not designed as an integral test facility, so will not match the dynamic response of the FHR. However, it is procedurally possible to perform a similar type of test for the DHX branch by using a pump trip and simulated power excursion/decay heat curve if a data set from an additional experimental facility is desired.

Because UNM's facility is designed to perform SETs on heat exchanger performance over a range of conditions, it would be an excellent facility to produce an SET benchmark focused on heat exchangers. At this point in the technological maturity of the concept, it is unclear which types of computer codes will be used to design a heat exchanger for an FHR. It may be possible to use some commercial codes for certain forced convection analyses, but these off-the-shelf codes will likely not be able to accurately capture the buoyantly-driven flow modes (for some discussion in the context of liquid-metal cooled reactors, see [17]) expected during LOFC transients or capture freezing phenomenology anticipated in TCHX cold spots during long outage scenarios. Because the DHX and TCHX will be designed to operate during passive flow conditions (and potentially near the salt freezing point under certain scenarios), it is likely that new code capabilities will need to be developed in the design space for FHR heat exchangers. Given that licensing is based in part on thermal-hydraulic safety codes used to analyze system behavior (integral level prediction) (for brief descriptions of computer codes used by the NRC, see [18]), it will ultimately be especially important to provide a benchmark that can be used in validation of system-level codes (e.g. RELAP5-3D, etc.). UNM will be acquiring high-quality heat transfer data for plain-tube and twisted-tube heat exchanger bundle performance assessment during natural and forced circulation that can be used for validation purposes. Data currently collected includes temperatures, flowrates, loop pressures, and current and voltage supplied to the heater, with the heat exchanger shell designed for measuring pressure drop through the bundle for the future addition of differential pressure transducers. In addition, it may be possible to do low power freezing tests in the heat exchangers by making small modifications to the experimental setup. These measurements lend themselves nicely to validation of systems-based codes, and will generate data that can be used to improve the fidelity of these codes (such as correlation development that could ultimately be incorporated in a systems-based code). They are also the types of measurements useful for validating FHR heat exchanger design codes when they become available.

At this point, it is also worth noting the increasing role that computational fluid dynamics (CFD) has recently seen in aiding heat exchanger design as the capability of computational resources and model development has improved (for a few examples, see [19], [20], [21]). CFD represents a more bottom-up approach to physics prediction, where the basic conservation equations are solved. This approach seeks to minimize the number of empirically-derived correlations/coefficients employed in the solution approach. Generally speaking, turbulence models utilize varying degrees of experimental data in their development, but at a lower level then systems-based codes. For example, a systems-based code will utilize integrated loss coefficients in predicting pressure drop (high-level/integrated effects), but a turbulence model in a CFD code will utilize closure correlations for modeling eddy behavior (low-level/local effects) to simulate the same problem. Because full-scale heat exchangers for power plants incorporate very complicated geometry utilizing thousands of tube to realize thermal duties in the megawatt range, heat exchanger sizing and general design will most likely be performed using specialized codes as discussed above.

However, as computational resources and CFD capabilities increase, it is very possible that CFD will be used to aid in understanding localized effects during the design process. From this perspective, two levels of SET benchmarks can be proposed: in addition to the benchmark described above, which could be considered as a mid-level/component benchmark, a second SET benchmark can be proposed for validation of CFD (low-level/SET benchmark). Because of the relative parameter detail required, a benchmark experiment aimed at satisfying the validation needs of CFD would likely not look at a heat exchanger bundle initially (due for example to difficulty in geometry characterization, computational burden, and uncertainty quantification). A better approach would be incrementally increasing complexity from the bottom-up. Such a benchmark could be based around simplified geometries utilizing a single tube, while increasing the phenomenological complexity in steps:

1. Single tube tests
    a. Plain tube
        i. Forced convection heat transfer (bi-directional)
        ii. Natural convection heat transfer
        iii. Heat transfer with freezing
    b. Enhanced tube (e.g. twisted tube)
        i. Forced convection heat transfer (bi-directional)
        ii. Natural convection heat transfer
        iii. Heat transfer with freezing
2. Multi-tube tests (e.g. 3 tube bundle)
    a. Plain tubes
        i. Forced convection heat transfer (bi-directional)
        ii. Natural convection heat transfer
        iii. Heat transfer with freezing
    b. Enhances tubes (e.g. twisted tubes)
        i. Forced convection heat transfer (bi-directional)

ii. Natural convection heat transfer

iii. Heat transfer with freezing

This approach would aid in identification of those components of the CFD model that may need improvement by separating local effects. If utilizing simulant fluids, it may be possible to acquire data for a large number of experimental runs due to the relative experimental simplicity and cost of testing a single or low number bundle of tubes. Data from such a set of experiments could also help indicate where additional validation data between simulant/prototypical fluids are needed. In addition, it is possible to do a higher level of instrumentation when testing a single tube or unit cell. This is because the geometry of a bundle limits the types of data/observations that can be made on the central tubes due to limited access. For example, with a single tube or unit cell bundle, it is possible to perform particle image velocimetry (PIV) measurements over a much larger fraction of the flow field than would be possible in a higher-number tube bundle. While UNM's heat transfer facility is not currently outfitted with a single/low tube count test section or PIV measurement system, it could be modified to perform these types of benchmarks.

4 Integral Effects Test Research Program

Integral effects tests (IETs) are an important class of thermal hydraulic experimentation that will be very valuable in understanding FHRs and validating system codes for FHR development. This chapter further explores the purpose of IETs in the context of this IRP's benchmarking efforts and details IET facilities that are available resources within the IRP.

4.1 Purpose of Integral Effects Tests

A key issue in designing and licensing new reactor designs, particularly those implementing passive safety, is the ability to validate integral thermal hydraulics transient response simulation codes. Models for pressure drop, heat transfer, and other phenomena used in thermal hydraulics transient codes are generally able to be validated using separate effect test (SET) experiments, where initial and boundary conditions are generated externally and can be varied across wide ranges. However, the idealized initial and boundary conditions in SETs may not adequately capture the actual initial and boundary conditions in an integral system due to the coupling between spatial regions and the transitions from early phases of transients to later phases of transients. To adequately capture the transient response of a complex, integral system, an integral effects test (IET) facility may be required to generate the representative data required to validate thermal hydraulics transient response simulation codes.

The importance of IET facilities' ability to capture the integral thermal hydraulic transient responses of complex system has been well understood for some time, especially in the nuclear reactor community. IET facilities tend to be scaled-down models of the systems that are representing; as long as initial and boundary conditions are scaled properly, data from IETs will represent the actual system response and can be used for code validation, proof-of-concept for innovation, and even for design licensing.

Internationally, there has been considerable effort in the development of IET facilities aimed at solving open issues for current reactors and nuclear power plants, for demonstrating the technical feasibility of new designs, and for model validation and benchmarking. In the United States, one IET facility stands out for its support of licensing by the US Nuclear Regulatory Agency (NRC). The APEX facility, located at Oregon State University, was used for confirmatory integral testing of passive safety systems of the Westinghouse AP1000. The NRC sponsored eight beyond-design-basis accident tests to confirm AP1000 safety margins and provide a database to assess NRC's thermal hydraulic computer codes. The NRC's review of the APEX-AP1000 test results showed conclusively that the reactor remains cooled without experiencing heat-up for most of the beyond-design-basis accident scenarios, and the NRC was thus able to conclude that Westinghouse's application for AP1000 design certification met the applicable content and standards of 10 CFR 52.47 and 10 CFR 42.48 [22]. The importance of IET data in the acceptance of the AP1000 design certification is a tremendous addition to the power and credibility of IET facilities and strengthens the role they play in the study and development of advanced reactor designs.

The same application of IETs towards the understanding, development, and licensing of light water reactors is applicable in the advanced reactor design space. The development and implementation of molten salt IETs is considerably more than for their light water counterparts. Major challenges with working with molten salt include heating the salt, keeping the salt from freezing, corrosion concerns for the system and for the salt purity, and compatibility of the salt with pumps, valves, gaskets, and other piping components.

4.2 University Integral Effects Test Experiments

The universities engaged in research within this IRP or as a partner include UCB, UW, and OSU. Each university hosts one or more facilities or research efforts to study the integral performance of molten salt systems, particularly FHRs.

4.2.1 University of California, Berkeley

UCB designed the first iteration of the compact integral effects test (CIET) facility (CIET 1.0) to reproduce the integral transient thermal hydraulic response of FHRs under forced and natural circulation operation [23]. CIET 1.0 provides validation data to confirm the predicted performance of the DRACS in FHRs. The facility has two coupled flow circuits: the primary coolant flow circuit, which replicates the main and bypass flow paths shown in Figure 21, and the DRACS circuit. The two flow circuits exchange heat through the DHX. The facility uses Dowtherm A as a simulant fluid for flibe, at reduced geometric and power scales. Test loops for CIET 1.0 were fabricated from thin-walled (schedule 10) 304 stainless steel (SS) pipe and butt-welded fittings to minimize the mass and thermal inertia. The favorable power scaling with oil (10 kW into oil being equivalent to 625 kW into flibe), along with the simplicity of the construction for low-temperature operation compared to the complexity and safety requirements for tests with the prototypical salt and other prototypical reactor coolants, were a key element in enabling the CIET 1.0 facility to be constructed at much lower cost than previous IETs for other reactor classes.

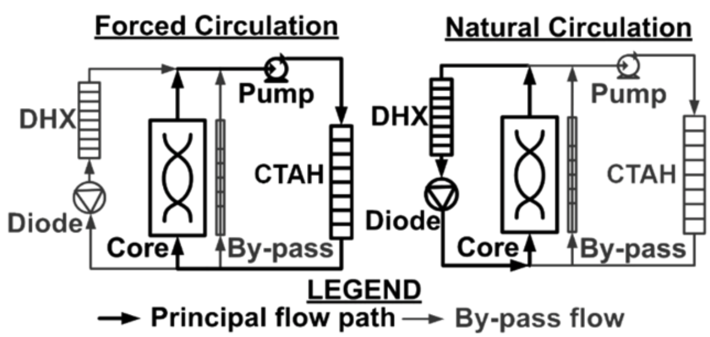

Figure 21. FHR Primary Coolant Flow Paths for Forced and Natural Circulation Operation.

Because the designs of FHR commercial prototype reactors will evolve, inherent distortions will exist between the CIET 1.0 facility and future FHR commercial prototype reactors. For transient response, such distortions may arise from non-matched relative coolant residence times between future FHRs and CIET 1.0 sub-systems, as well as the use of reduced flow area SS piping with non-scaled thermal inertia in CIET 1.0. However, while CIET 1.0 was scaled based on the earlier design of a 900-MWth channel-type pebble-bed advanced high-temperature reactor (PB-AHTR), and the pre-conceptual design of a 236-MWth Mk1 PB-FHR was completed after scaling and design of CIET 1.0 were already finalized, elevations of the main heat sources and sinks in CIET 1.0 and the Mk1 PB-FHR design reveal a reasonable agreement between the scaled model and prototype. Therefore, CIET 1.0 will provide useful validation data for integral transient behavior of a generic set of FHRs, and given the low cost of the CIET facility, final code validation for a future commercial prototype plant would likely include construction of a new CIET-type loop scaled to closely match the prototypical design.

For lack of detailed heat exchanger designs when scaling was performed and design decisions were made for CIET 1.0, the heat exchangers in the system are not scaled to any prototypical heat exchanger. Instead, their designs are based on functional requirements in terms of heat transfer performance, and only relative elevations of the heat sources and sinks are scaled to the 900-MWth modular PB-AHTR. However, the ability to control fan speeds on the two oil-to-air heat exchangers using variable frequency drives (VFDs), as well as to interchange the current oil-to-oil heat exchanger that couples the primary and DRACS flow loops with another scaled heat exchanger design, leaves great flexibility in heat removal options for the CIET 1.0 system. Similar to the heat exchangers, the primary pump on CIET 1.0 is not scaled to any prototypical pump. Instead, its design is based on functional requirements in terms of pump head and resulting flow rates in the system. All instrumentation, as well as the computer-controlled power supply and VFDs are integrated through the LabVIEW software and manually or automatically controlled from a central computer station. Figure 22 shows the computer-aided design rendering of the CIET 1.0 loop with the main components labeled.

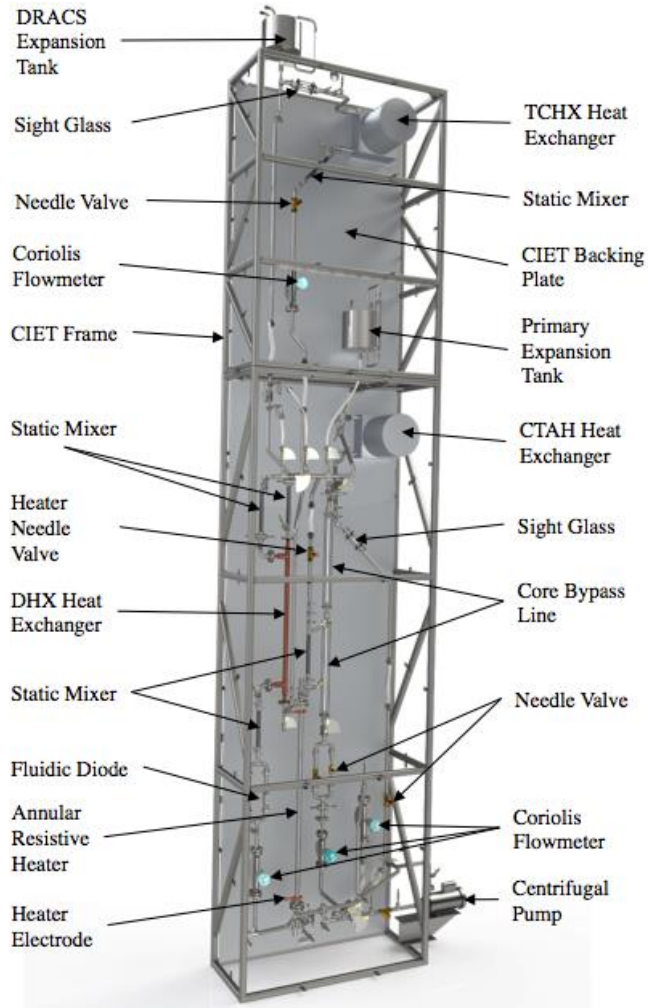

Figure 22. 3D rendering of the CIET 1.0 facility.

Between 2011 and 2014, CIET 1.0 was designed, fabricated, filled with Dowtherm A oil and operated. Isothermal pressure drop tests were completed, with extensive pressure data collection to determine friction losses in the system. CIET-specific friction loss correlations were compared with handbook values, and empirically measured values were implemented in the system codes that are to be validated by CIET data. The project then entered a phase of heated tests, from parasitic heat loss tests to more complex feedback control tests and natural circulation experiments. In parallel, UCB has been developing thermal hydraulic models to predict FHR steady-state characteristics and transient response for a set of reference LBEs. The general strategy is to rely on existing general-purpose thermal hydraulic codes with a significant V&V basis for design and licensing by the U.S. Nuclear Regulatory Commission, such as RELAP5. However, UCB has also been developing a one-dimensional FHR advanced natural circulation analysis (FANCY) code for CIET 1.0 and FHR natural circulation modeling. FANCY results will be compared with RELAP5 and validated by data from CIET 1.0. Validation data will include steady-state forced and coupled natural circulation data in the primary loop and the DRACS loop, and thermal transient data (e.g., startup, shutdown, loss of forced circulation with scram and loss of heat sink with scram).

Current research focuses on validation and verification of some of the major transient scenarios listed above, particularly for the loss of forced circulation and loss of heat sink scenarios. Additional physical modifications to the facility include active guard heating to reduce parasitic heat losses, an advanced internal structure in the heating element to promote enhanced heat transfer, and an upgraded system control architecture to approach the general capabilities of modern reactor simulator facilities.

4.2.2 University of Wisconsin, Madison

Research efforts in the area of integral effects at UW-Madison include the UW flow loop, research in natural circulation stability, and a more thorough scaling analysis of freezing of liquid in a pipe and how this phenomenon may be important for IETs.

4.2.2.1 UW Flow Loop

The UW Flow Loop is a FLiBe thermal convection loop designed for dynamic flow corrosion testing. Before testing corrosion samples, a battery of thermal-hydraulic tests will be performed to characterize the flow environment and provide data that could be used for future code verification or scaling analysis. The loop design is based on historic loops from the MSRE project and expects to operate around 700 – 800 °C with flow velocities around 5 cm/s.

The flow loop design, shown in Figure 23, follows the same basic layout as previous MSRE corrosion flow loops. In addition to controlling power input to the radiant mode heaters, the loop can also control the forced convection cooling through a blower system that forces air through the two annular coolers on the top and down-comer legs. The loop temperature is monitored by both wetted and dry thermocouples mounted at numerous points around the loop and additionally by a fiber optic temperature sensing cable that will be installed for the thermal-hydraulic testing phase. During this time, both vertical legs will be instrumented with two fiber optic temperature sensors; one in the tube center and the other in a groove cut into the outer edge of the tube wall. These fibers were installed due to concerns about the extreme temperature gradient reducing the accuracy of single point thermocouple readings due to large amounts of heat conduction along the thermocouple's sheath. Additionally, the loop carries two redox probes for measuring salt chemistry during corrosion testing, but does not carry a flow meter, because no suitable flow meter could be found for the necessary operating conditions and geometric constraints. Instead, flow measurements will be derived by heating a section of piping and measuring the hot salt's transit time between two thermocouples.

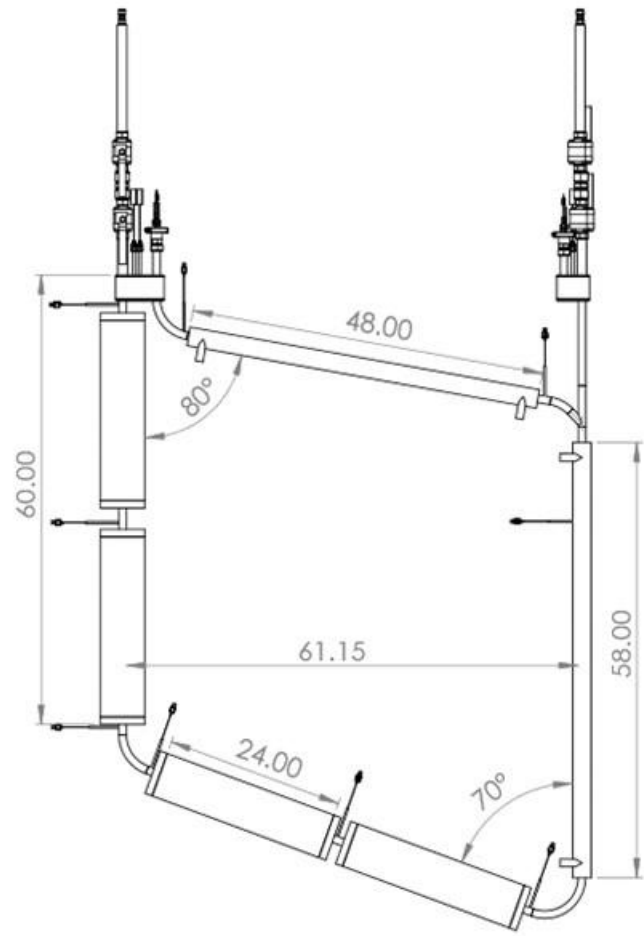

Figure 23. Schematic of the UW flow loop.

Concurrent with construction, the flow loop has also been modeled using the Computational Fluid Dynamics (CFD) code ANSYS Fluent; which has provided some unique operating predictions. Most importantly, ANSYS Fluent results have indicated that the low thermal conductivity of the salt will result in extreme flow stratification; a nearly stagnant, isothermal core of salt surrounded by a higher velocity annulus near the pipe walls. This stratified flow is undesirable for a number of reasons, including reducing the heat transfer capabilities of the salt, one of its key characteristics in its selection for the FHR. This could be an important phenomena for design of the emergency heat removal systems of the FHR, which rely heavily on natural circulation. However, the simulations thus far have been limited in scope. Fully system simulations have utilized two-dimensional representations of system piping, which seems to exaggerate the flow stratification. Further simulations are being undertaken to provide more realistic validation of the loop piping and planned experimentation will measure temperatures with the goal of understanding the flow fields for comparison against CFD results.

4.2.2.2 Natural Circulation Stability

Natural circulation systems offer a very convenient option of efficient passive energy transport to remove decay heat from the reactor core under certain normal operating conditions or in a shut-down. In general, natural circulation systems are more unstable than forced circulation systems due to the nonlinear nature of the natural circulation mechanism and its low driving force. The Heat and Mass Transport group at the University of Wisconsin at Madison is currently working on the stability behavior of natural circulation in FHR. A 1-D transient study has been conducted in COMSOL Multiphysics for a simple molten salt natural circulation loop with uniform heat fluxes at the cooled and heated sections of the loop. All the remaining sections of the loop were assumed perfectly insulated. Moreover, the pipe wall is assumed to have negligible thermal resistance and radiant heat transfer is neglected. The momentum and energy balance equations of the natural circulation were numerically solved in COMSOL using temperature-dependent thermo-physical properties for FLiBe. The simulation results predict that the system reaches a periodic-steady-state condition and the period of the waveform is equivalent to the amount of time it takes for the salt to complete one loop, as shown in Figure 24. The cyclic behavior is attributed to the absence of any environmental influences from the system's surroundings due to the uniform heat addition and extraction at the heated and cooled sections of the loop which causes the formation of hot and cold pockets that travel along the loop in a cyclic manner. Further simulations showed that a constant convective boundary condition at the cooled section of the loop instead of a uniform wall heat flux condition has an attenuating effect on the cyclic behavior of the flow/temperature in the system, as shown in Figure 25.

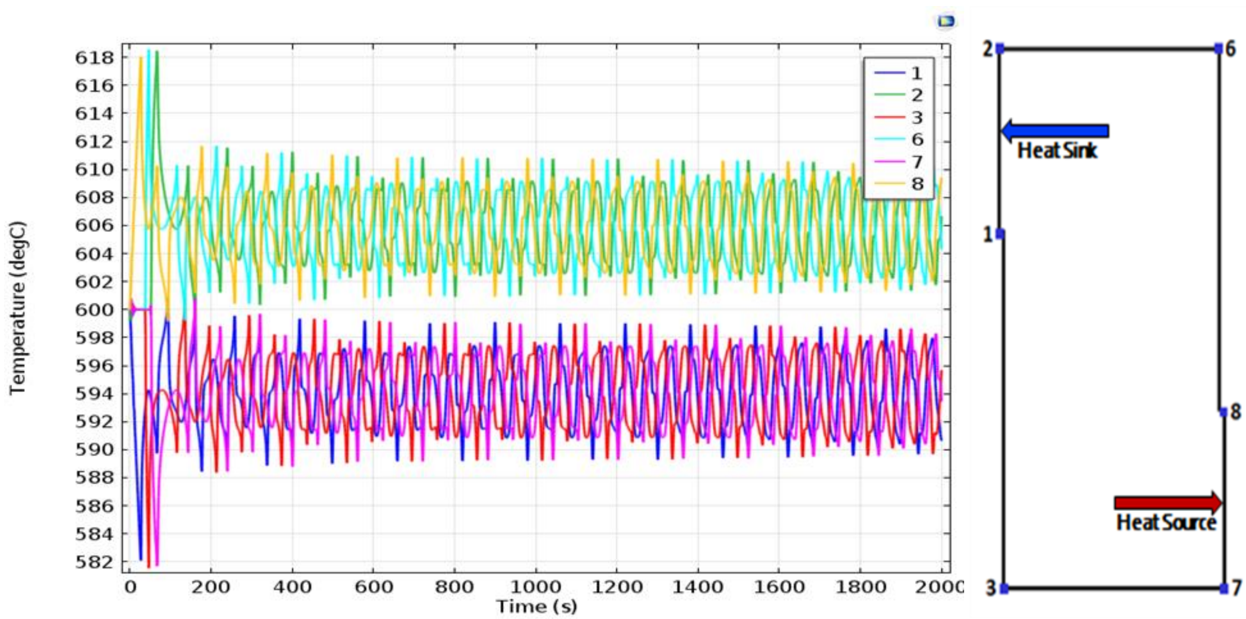

Figure 24. Temperature of salt versus time at different locations in the natural circulation loop for the case of a uniform heat flux at the cooled section.

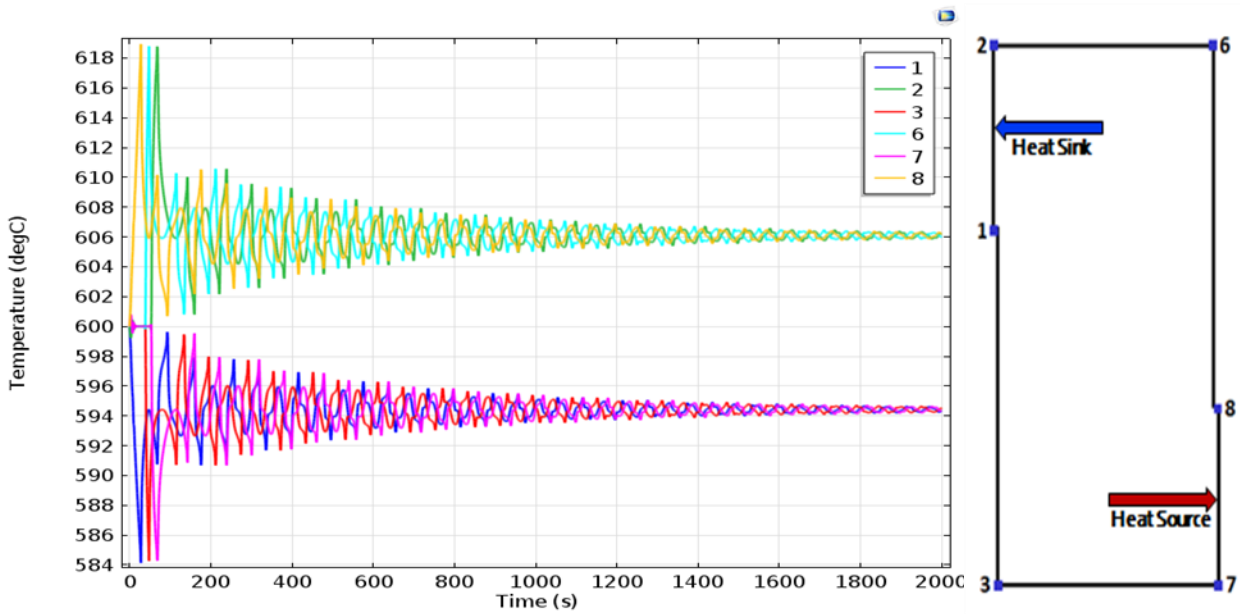

Figure 25. Temperature of salt versus time at different locations in the natural circulation loop for the case of a constant convective boundary condition at the cooled section.

A 1-D linear stability analysis is currently being performed for a single-phase molten salt natural circulation loop that uses FLiBe as the coolant. The Nyquist Stability Criterion is employed to estimate the stability boundary of the closed loop system. This technique is an effective frequency domain analysis technique that can provide us with information on the stability conditions for any given Reynolds Number. Using this technique, we can estimate the critical Grashof number for a given Reynolds number for the steady-state solution to become unstable. Figure 26 shows the stability boundary at Re = 92 and heat source of 1000 W/m. The solid curve in the $F(w)$ plane is mapped to the positive imaginary branch of the closed curve in the w-plane, whereas the dotted line corresponds to the negative branch. The figure shows that the curve in the $F(w)$ plane does not enclose the origin, and therefore the steady state solution is stable in this case.

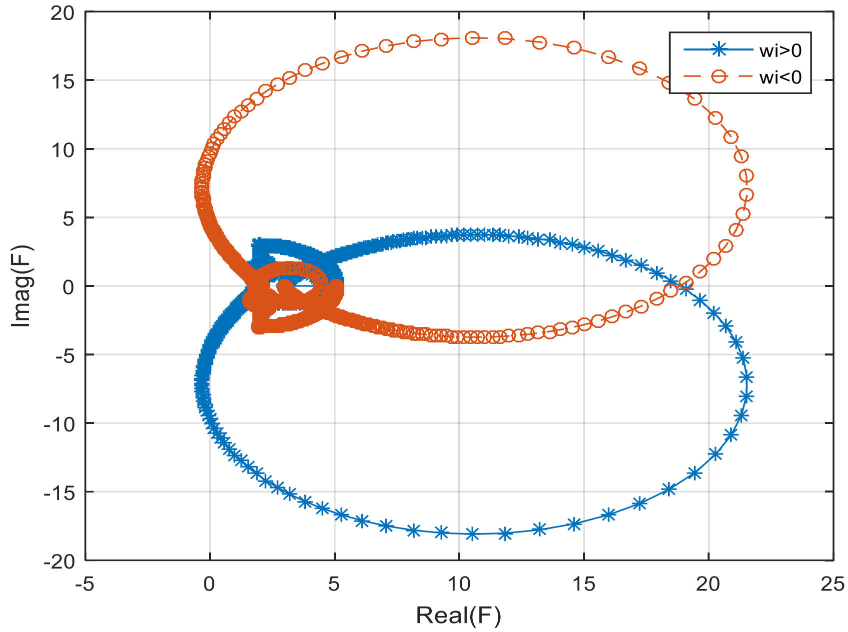

Figure 26. Stability boundary at Re = 92 and heat source of 1000 W/m.

For future work, it is important to include the thermal inertia of the pipe wall in the model as well as heat losses through pipe wall insulation which is presumed to have a significant effect on the oscillatory behavior. For the natural circulation stability studies, the 1-D model can be extended to relax some of the assumptions, for example, consideration for a mixed boundary condition; radiative and convective heat transfer at the cooled section of the loop. Moving forward, the ultimate goal is to develop a working model that investigates the effect of freezing of salt on the stability of the natural circulation in the DRACS. To capture this effect, the loop response to the disturbances caused by the freezing problem can be expressed in the form of pressure drop or changes in the velocity profile. Another goal is to investigate the loop stability problem when considering multiple branches of the heat exchangers.

4.2.2.3 Scaling Analysis of Freezing of Liquid in a Pipe

Another part of our current work at the University of Wisconsin at Madison is to scale FLiBe freezing in pipe flows with FLiNaK and Dowtherm A as simulant fluids. The flow response to this disturbance is one of the foremost interests in conducting this work. A 1-D scaling analysis of freezing of liquids in a pipe has been conducted to study the freezing problem in pipe flows in the FHR heat exchangers (TCHX, DHX and CTAH). From this analysis, a set of scaling arguments has been identified for the scaled comparison of different liquids:

Reynolds: $$Re = \frac{2\rho_L \bar{u}_0 R}{\mu} \quad (1)$$

Prandtl: $$Pr = \frac{c_L \mu}{k_L} \quad (2)$$

Stefan: $$Ste = \frac{c_S (T_o - T_f)}{H_f} \quad (3)$$

Heat Flux Parameter: $$\Pi_Q = \frac{\dot{q}_w''}{k_S(T_o - T_f)/R} \quad (4)$$

Thermal Conductivity Ratio: $$\Pi_k = \frac{k_L}{k_S} \quad (5)$$

Aspect Ratio: $$\Pi_R = \frac{R}{L} \quad (6)$$

In our analysis, the liquid is assumed Newtonian, incompressible, and a pure substance. The flow is assumed everywhere laminar and radiant heat transfer and free convection were considered negligible. We also assumed a constant pipe wall heat flux, inlet temperature, and velocity. Furthermore, a quasi-steady state assumption is made that the bulk temperature of the fluid and the solid layer temperature reach a steady state distribution instantly as the freeze-front position changes with time and axial distance. Table 2 summaries the FHR heat exchangers parameters on the FLiBe side for a single tube for the Coiled Tube Air Heater (CTAH), the DRACS Heat Exchanger (DHX) and the Thermosiphon-Cooled Heat Exchanger (TCHX), for the Mark 1 PB-FHR design. Using these dimensionless arguments, experimental parameters to study the freezing of FLiBe in FHR can be determined. A pipe freezing model and experiment should be able to vary all of the parameters to determine their effect on the freeze layer profile and heat transfer profile. Table 3 shows the scaled TCHX parameters required to model a single tube in the TCHX using FLiNaK and Dowtherm A for a length scale of 1:1. These parameters would be necessary to use in a pipe freezing experiment in which the reactor in shutdown mode were to be modeled.

Table 2. Mark-1 PB-FHR design parameters for the CTAH, DHX, and TCHX.

Parameter	CTAH	DHX	TCHX	Unit
Minimum Temperature	600	526	526	°C
Mass Flow Rate	0.0351	0.0121	0.051	kg/s
Inlet Velocity	1.08	0.0641	0.27	m/s
Inside Diameter	0.00457	0.0109	0.0109	m
Tube Length	18.47	24.0	24.0	m
Tube Wall Heat Flux	25.37	24.08	10.54	kW/m^2
Reynolds	1189	119.0	500.5	-
Prandtl	18.64	27.88	27.88	-
Stefan	0.452	0.215	0.215	-
Reynolds at freezing point	562.9	81.38	342.2	-
Prandtl at freezing point	42.15	42.15	42.15	-

Table 3. Scaled TCHX parameters for FLiNaK and Dowtherm A for a length scale of 1:1.

Parameter	FLiBe	FLiNaK	Dowtherm A	Unit
Inlet Temperature	526	641	26	°C
Freezing Point	459	454	12	°C
Mass Flow Rate	0.051	0.0143	0.0172	kg/s
Inlet Velocity	0.27	0.0742	0.175	m/s
Inside Diameter	0.0109	0.0109	0.00109	m
Tube Length	24.0	24.0	24.0	m
Tube Wall Heat Flux	10.54	22.69	0.3009	kW/m^2
Reynolds	500.5	500.5	500.5	-
Prandtl	27.88	7.282	46.36	-
Stefan	0.215	0.215	0.215	-

For future work, we are going to expand our scaling analysis by considering two different initial conditions; hydrodynamically and thermally fully developed flow versus hydrodynamically and thermally developing flow which has an increasing frozen layer starting from zero thickness at the inlet. Furthermore, two different boundary conditions will be explored; constant wall temperature and uniform wall heat flux.

Table 4 shows the empirical correlations used to determine the temperature-dependent thermophysical properties for liquid FLiBe, FLiNaK and Dowtherm A. It is noteworthy that the thermophysical properties for the solid phase were determined from the available liquid correlations by extrapolating to the freezing point. The enthalpy of fusion for FLiBe and FLiNaK were determined by taking the weighted average of the enthalpy of fusion of their components (LiF-BeF2 for FLiBe and LiF-NaF-KF for FLiNaK).

Table 4. Liquid thermophysical properties for FLiBe, FLiNaK, and Dowtherm A.

Property	Correlation	Unit
FLiBe (Temperature in °C in the range of 600 to 800 °C)		
Viscosity	$4.638 \cdot 10^5 / T^{2.79}$	Kg/m-s
Specific Heat	2415.78	J/kg-K
Thermal Conductivity	$0.7662 + 0.0005 \cdot T$	W/m-K
Density	$2279.92 - 0.488 \cdot T$	Kg/m^3
FLiNaK (Temperature in K in range of 770 to 1170 K)		
Viscosity	$2.487 \cdot 10^{-5} \cdot \exp(4478.62/T)$	Kg/m-s
Specific Heat	1905.57	J/kg-K
Thermal Conductivity	$0.36 + 0.00056 \cdot T$	W/m-K
Density	$2729.3 - 0.73 \cdot T$	Kg/m^3

Dowtherm A (Temperature in °C in the range of 20 to 180 °C)		
Viscosity	$0.130/T^{1.072}$	Kg/m-s
Specific Heat	$1518 + 2.82 \cdot T$	J/kg-K
Thermal Conductivity	$0.142 - 0.00016 \cdot T$	W/m-K
Density	$1078 - 0.85 \cdot T$	Kg/m^3

In order to conduct an effective scaling analysis, it is important to use accurate data of the thermo-physical properties of the different fluids being investigated, especially near their freezing points. We will need data of the different physical properties (density, thermal conductivity, specific heat) before, during and after the liquid-to-solid change of phase. We also need data on the enthalpy of fusion of these different liquids. Different research groups and universities will also need to work together on identifying a consistent set of data for the thermo-physical properties of such fluids and their uncertainties that can be implemented in all experimental and simulation codes and models.

4.2.3 The Ohio State University

OSU has two primary IET facilities to study the performance and optimization of the DRACS system within FHRs. The two IET facilities are the Low-Temperature DRACS Test Facility (LTDF) and the High-Temperature DRACS Test Facility (HTDF).

To experimentally investigate the DRACS thermal performance, two test facilities, namely, a LTDF and a HTDF have been designed and constructed at The Ohio State University (OSU). Both of the LTDF and HTDF are scaled down from a 200-kW prototypic DRACS design for a pebble bed reactor design, by following a rigorous scaling analysis [24]. The LTDF uses water as the surrogate coolants and is intended to investigate the couplings among the loops/subsystems of the DRACS, as well as providing useful design, construction, and operation experience for the HTDF. The HTDF employs FLiNaK and KF-ZrF_4 as the primary and secondary coolants, respectively. With the HTDF, the DRACS performance in terms of its capability of removing decay heat under prototypic reactor conditions can be evaluated.

4.2.3.1 Low-Temperature DRACS Test Facility (LTDF)

The LTDF constructed at the OSU is shown in Figure 27, Figure 28, and Figure 29. The LTDF uses water as the surrogate coolant for both the DRACS primary and secondary loops. The main components involved in the LTDF include a simulated core, DHX, NDHX, fluidic diode simulator, secondary throttling valve, pump, accumulator, air chimney system, and primary and secondary water tanks.

Figure 27. Image of the LTDF on the OSU campus.

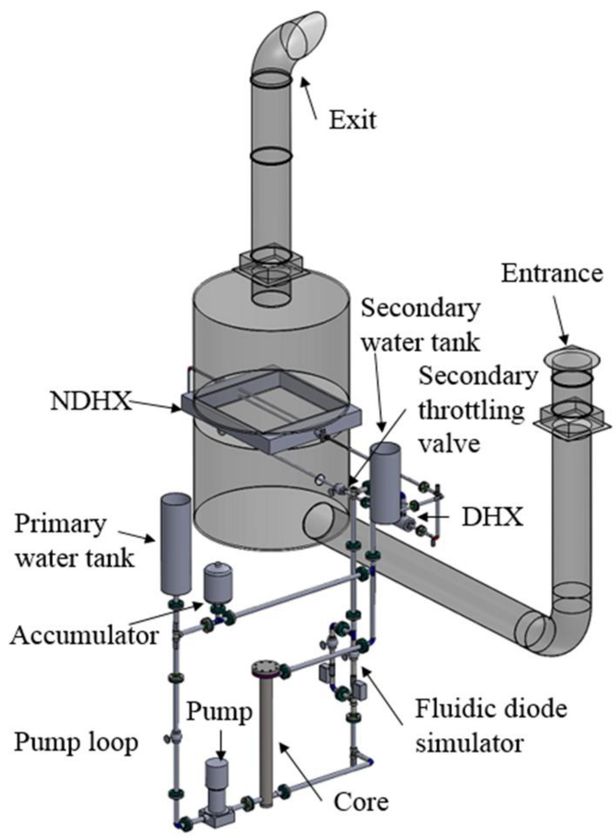

Figure 28. Three dimension CAD model of the facility layout.

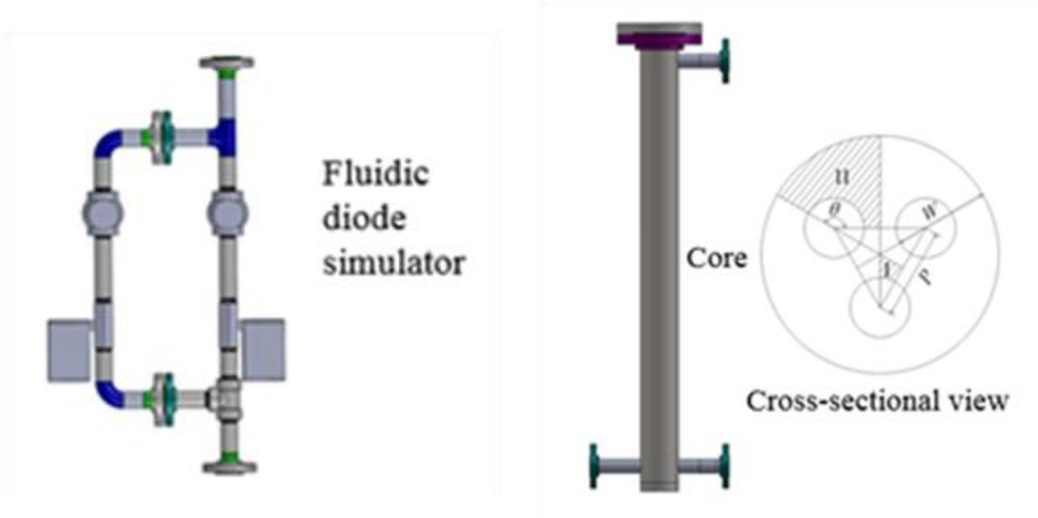

Figure 29. Model of the LTDF simulated core and the fluidic diode simulator.

The simulated core consists of three cartridge heaters that are arranged in a triangular pattern and surrounded by a cylindrical vessel, as shown in Figure 29. Each heater has a nominal power capability of 2 kW, totaling up to 6 kW for the entire core. During operation, the heater sheath surface temperature could exceed 100°C. To prevent any potential subcooled boiling from occurring in the simulated core, the primary loop and pump loop are pressurized to 1.0 MPa using a nitrogen-filled accumulator.

A shell-and-tube heat exchanger with one tube pass is adopted for the DHX. In the DHX, the pressurized primary water flows on the shell side while the secondary water is on the tube side. For the NDHX, to enhance the air-side heat transfer, a finned-tube heat exchanger with copper tubes and aluminum fins has been employed.

In the current LTDF, a combination of two globe valves and two ball valves is employed to simulate the fluidic diode, as also shown in Figure 29. The two parallel branches, each of which consists of a globe valve and a ball valve, simulate the forward and reverse flow directions of the fluidic diode. The two globe valves are identical, and can provide flow resistance as desired by turning the valve stem. The same globe valve is used as the secondary throttling valve to adjust the flow resistance in the secondary loop. The two ball valves are motorized, and only one of the two ball valves is open at a given flow direction.

A special air chimney design, utilizing the two existing penetrations in the laboratory roof as the entrance and exit, is adopted, as shown in Figure 28. The NDHX is placed between two large air ducts beneath the chimney exit. All the air ducts are thermally insulated with fiberglass and ceramic fiber blankets to maintain the incoming air temperature and inhibit heat loss from the hot leg where the hot air rises after passing through the NDHX.

The LTDF includes a pump loop that simulates the primary heat transfer loop in an FHR. A 2-hp vertical inline circulating pump is employed in the pump loop, enabling the study of the flow reversal phenomenon in the DRACS primary loop following a pump trip event associated with loss of power and reactor shutdown. A variable frequency drive is used to control the speed of the pump. Two water tanks are used to add water to the primary/pump and secondary loops, while the secondary water tank also serves as the expansion tank.

The LTDF is fully instrumented. Three clamp-on ultrasonic flow meters provided by Flexim are installed in the primary, pump, and secondary loops to measure the water flow rates. A thermal mass flow meter from Eldridge is employed for the air flow measurement in the air chimney, which employs a special averaging tube that reduces the required upstream straight pipe run and makes the measurement more accurate. A Honeywell differential pressure transducer is used to measure the pressure drops over the fluidic diode simulator and secondary throttling valve, which are the main pressure drop contributors to their respective loops. A Honeywell gauge pressure transducer is used to monitor the pressure of the primary/pump loop when being pressurized. T-type thermocouples from Omega Engineering are employed to measure the inlet and outlet temperatures of all the heat exchange components, namely, the core, DHX, and NDHX. Lastly, each of the three core heaters is individually controlled by an SCR controller to adjust the power, and the actual power provide to each heater is measured by a watt transducer. All the instruments have been calibrated using standards whose accuracies are traceable to NIST (National Institute of Standards and Technology) [25].

For illustrative purposes, one of the tests performed in the LTDF that studies the DRACS transient performance during a pump trip scenario is discussed here. In this scenario, a steady-state core normal operation is first simulated before initiating the accident transient. This simulated core normal operation is different from the prototypic core normal operation in that there is no IHX in the LTDF. Therefore, the LTDF simulated core will not provide the nominal core normal operation power but instead a power representing the parasitic heat loss to the DRACS during core normal operation. For the simulated core normal operation, a power of 2 kW is provided to the LTDF core. The pump speed is adjusted in conjunction with the opening of the globe valve in the reverse flow direction of the fluidic diode simulator so that the parasitic flow through the fluidic diode and the main flow through the core are approximately 0.04 and 1.68 kg/s, respectively, which are determined from the scaling analysis [12]. The system is maintained in operation until a steady-state is reached, following which the accident is initiated by shutting down the pump and switching the core power to the simulated decay heat, which also has a nominal value of 2 kW in this case. The initial parasitic flow through the fluidic diode simulator is constantly monitored, and when it decreases to zero, the branch representing the forward flow direction is opened and the other branch closed.

The evolution of the coolant temperatures and flow rates following the pump trip are shown in Figure 30 through Figure 34. As can be seen from Figure 30 and Figure 31, following the pump trip, the water temperatures in the primary loop experience an abrupt change due to the flow reversal, and then gradually decrease until a quasi-steady state is reached. The flow reversal in the primary loop also causes perturbations in the secondary loop coolant temperatures and air outlet temperature, which then decrease slowly until a new quasi steady state is reached. As can also be seen from Figure 30, the primary and secondary coolant temperatures and the air outlet temperature reached in the new quasi-steady state are lower than those reached during the core normal operation which is primarily due to the following three reasons. Firstly, the air inlet temperature has been constantly decreasing during the entire transient, as seen from Figure 30, since the experiment started in the afternoon. Secondly, the flow configuration in the DHX during the core normal operation is co-current flow, which is not as efficient in terms of heat transfer as the counter-current flow configuration in the eventual quasi-steady state, thus leading to higher primary coolant temperatures during the core normal operation. Lastly, although the simulated parasitic heat loss during the core normal operation and the decay heat during the DRACS transient operation have the same nominal value of 2 kW, due to the pump heating, the actual heat transferred by the DRACS during the core normal operation is higher, which also explains the decrease in the secondary flow following the pump trip shown in Figure 32. The air flow rate, seen from Figure 32, shows some fluctuations during the transient following the pump trip. This is found to be an effect by the external wind, as the cooling air is introduced into the LTDF directly from the ambient environment. It can be seen from Figure 33 and Figure 34 that, after the pump trip, the residual pump flow and the parasitic flow through the primary loop decrease to zero very quickly, mainly due to the large flow resistance in the loop and relatively small inertia of the pump. The primary water flow is seen to decrease to zero over approximately 5 seconds and start to develop in the reverse direction immediately. No significant period of time during which the primary flow is stagnant is observed during the flow reversal process, mainly due to the existing temperature gradient and corresponding buoyancy force in the primary loop when the pump is shut down. Lastly, a new quasi steady state is reestablished at approximately 17,500 seconds.

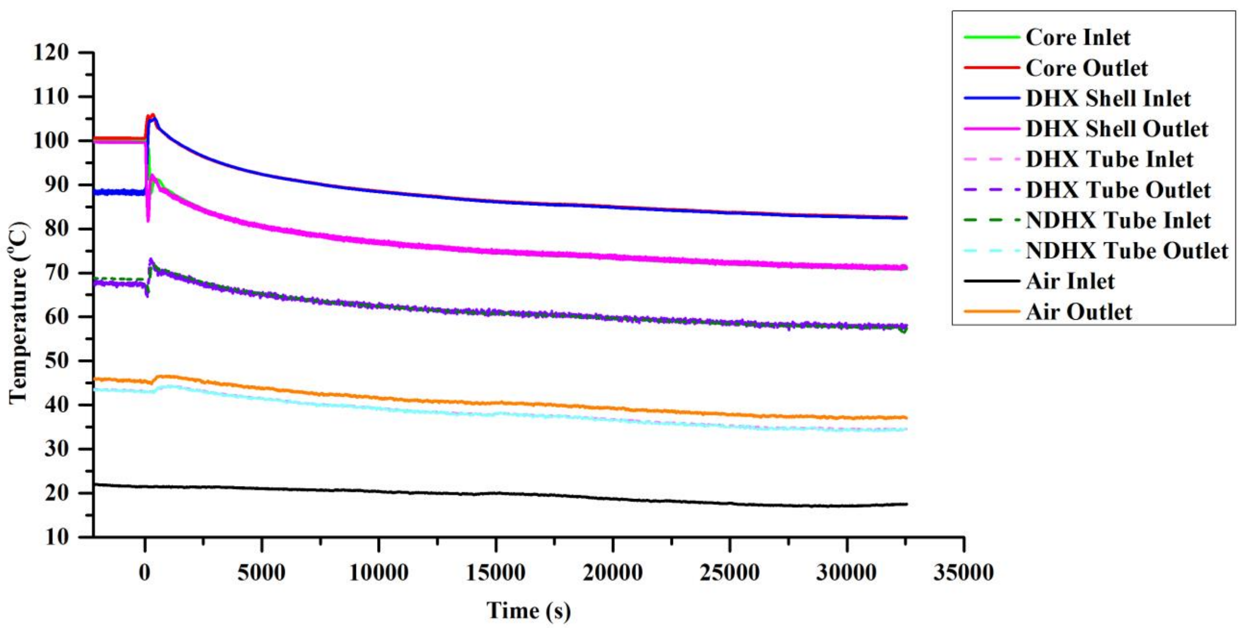

Figure 30. Overall development of fluid temperatures during the pump trip transient.

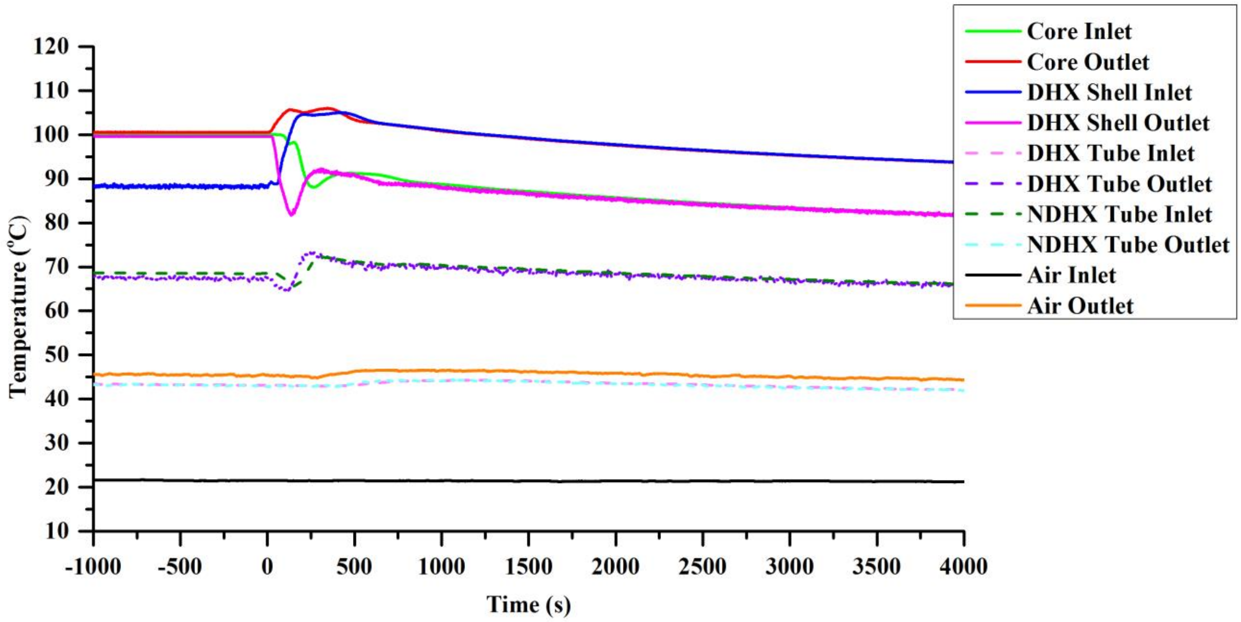

Figure 31. Zoom-in of the fluid temperature development during the pump trip transient.

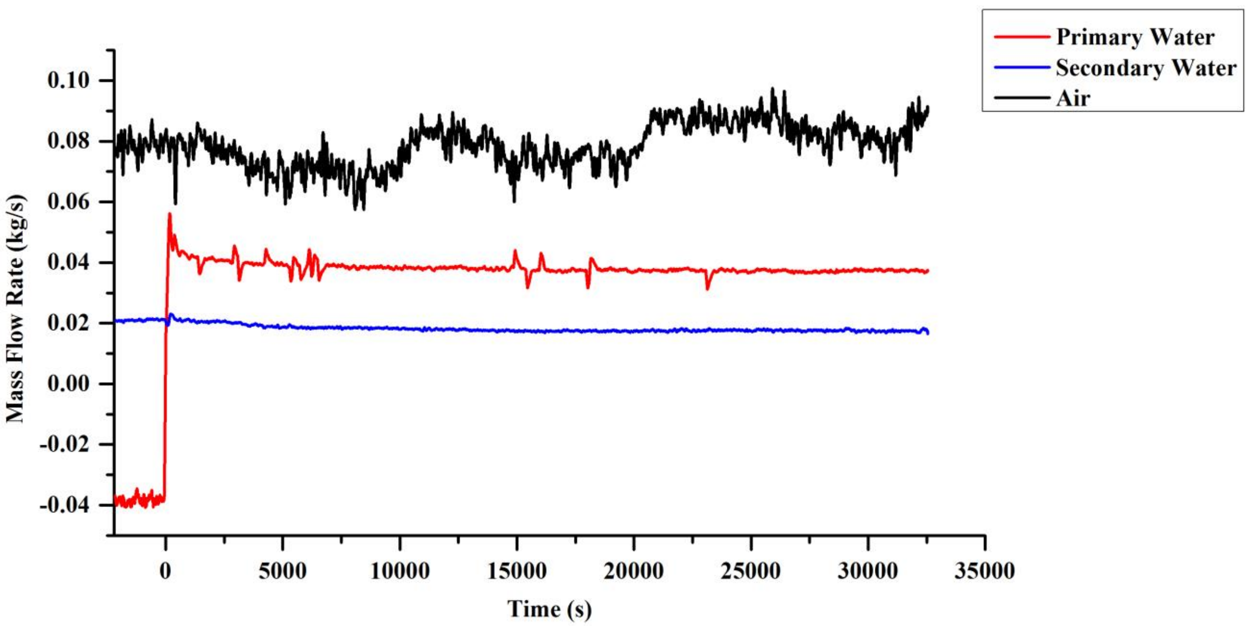

Figure 32. Overall development of the coolant flows during the pump trip transient.

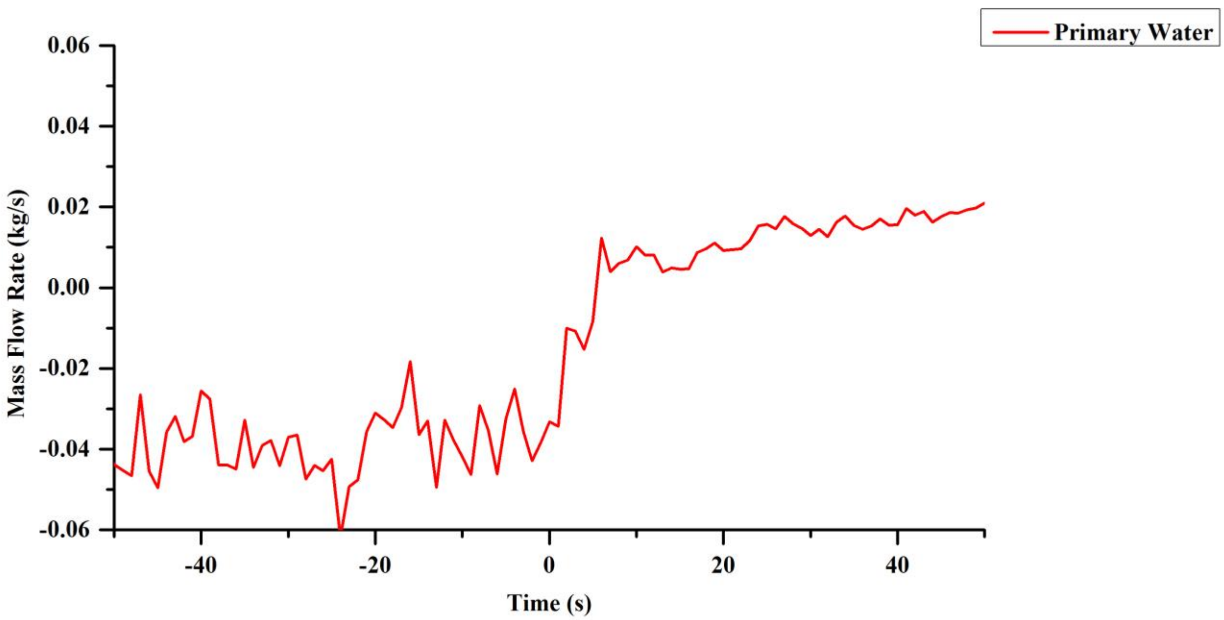

Figure 33. Primary flow reversal.

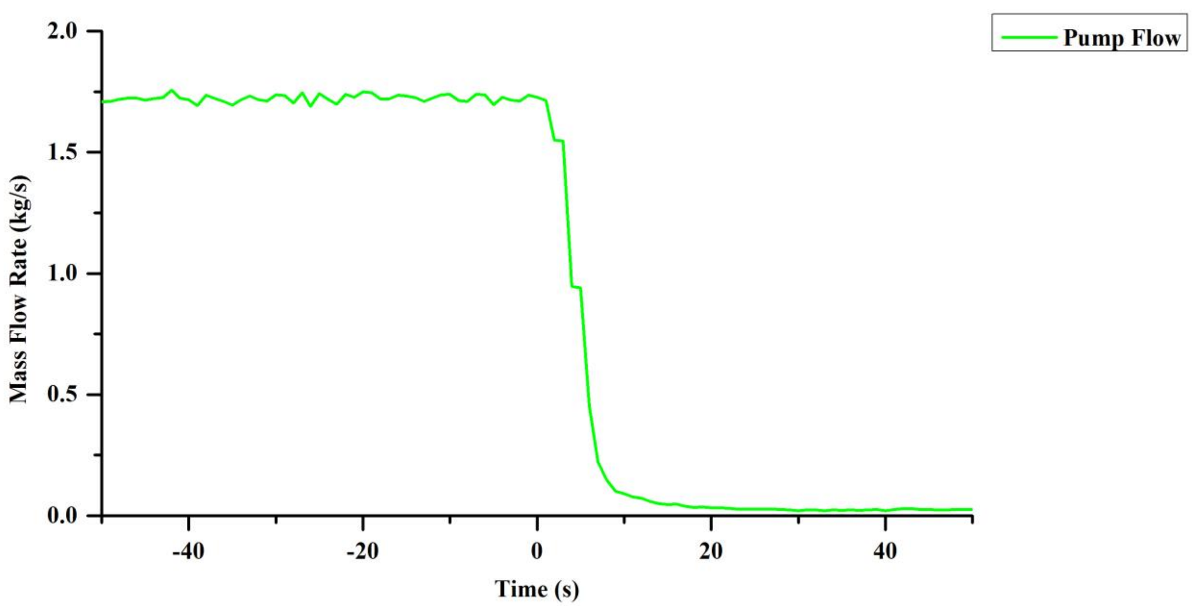

Figure 34. Pump trip curve.

4.2.3.2 High-Temperature DRACS Test Facility (HTDF)

The HTDF is constructed by the side of the LTDF, with the two facilities sharing the same chimney system. A three-dimensional schematic of the HTDF is illustrated in Figure 35. The HTDF employs FLiNaK and $KF\text{-}ZrF_4$ as the primary and secondary coolants, respectively. The major components in the HTDF primary and secondary loops are connected through 1-1/2” and 1-1/4” Sch 40 pipes, respectively. The HTDF core is simulated with 7 electric cartridge heaters with a total nominal power of 10 kW. The DHX employs a shell-and-tube heat exchanger design containing 80 5/8” BWG-18 tubes at a length of 0.325 m. Due to the large temperature difference between the secondary salt and ambient air, plain tubes are used for the NDHX. A total of 36 1/2” BWG-16 tubes are adopted in a staggered array in two rows. A vortex diode design that will exhibit desired pressure drop characteristics for both the forward and reverse flow directions has been obtained via a parametric CFD study [26]. The diode design employs converging/diverging nozzles and a disk-shape chamber with a diameter of 6.6 cm and thickness of 1.56 cm [29]. In addition, a cantilever sump pump for high-temperature applications has also been employed in the HTDF. The nominal design conditions for steady-state operation of the HTDF are summarized in Table 5.

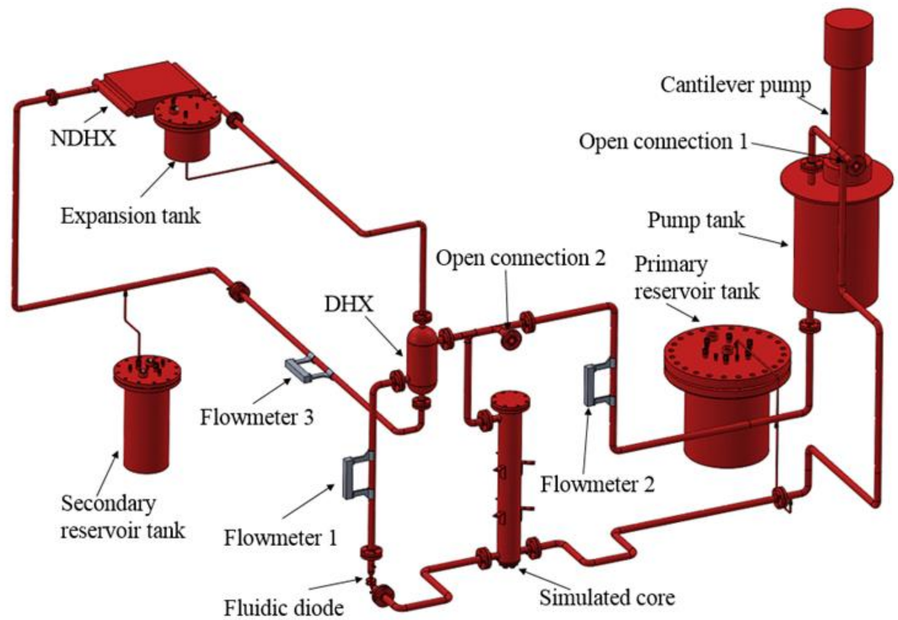

Figure 35. Three-dimensional representation of the HTDF.

Table 5. Nominal design conditions of the HTDF.

	Primary Salt (FLiNaK)	Secondary Salt (KF-ZrF_4)	Air
T_{hot} (°C)	722.1	665.3	110.0
T_{cold} (°C)	677.9	589.7	40.0
ΔT (°C)	44.2	75.6	70.0
$\dot{m}$ (kg/s)	0.120	0.127	0.142

The HTDF is fully instrumented with gauge pressure transmitters to monitor the cover gas pressure in all the salt tanks, capacitance level sensors to monitor the tank salt levels, and thermocouples (N-type) to measure/monitor the salt temperatures along the loop, as well as in the tanks. High-temperature clamp-on ultrasonic flow meters from Flexim are employed to measure the flow rates. The same flow meters have been provided to ORNL for a similar application with temperatures up to 700°C. For the differential pressure measurement, in-house designs utilizing commercial differential pressure transmitters have been developed, which require accurate control of the salt-Ar interface in the pressure sensing lines.

To ensure successful operation of the HTDF, tests including components test, leakage test, instrumentation test, and corrosion test will be necessary, mainly due to the challenges of the high temperatures and corrosion issues. Currently, two preliminary tests have been performed, while the other tests are still undergoing. The first test is on the salt preparation strategy while the second on the fabricated fluidic diode. The results from the two tests will be discussed in future reports.

4.3 Example Integral Effects Test Benchmark

In the previous workshop, two benchmarking exercises were suggested that are both applicable to IET facilities and simulations [16].

1. Candidate exercise one (CE1) explores steady-state natural circulation flow in a loop. The purpose is to validate the relevant performance models against experimental data for validation. This is a critical first step before more advanced models/scenarios can be explored. This exercise is able to be performed on many experimental facilities, including CIET 1.0, the UNM Heat Transfer Loop, thermal hydraulic loops developed at UW, the OSU DRACS test loops, the Liquid Salt Test Loop at ORNL, and the thermal hydraulic loops at SINAP. The ability to perform CE1 on several test facilities and validate several models should lead to very accurate and flexible natural circulation models. It is important to note that this is a relatively straightforward test to perform in isolation (without coordinated benchmarking with other universities or partners), and there may already be work underway or work completed that can be included in this effort.

2. Candidate exercise two (CE2) is meant to represent a mature benchmarking exercise that should be performed towards the end of the project after more fundamental areas are fully explored and essential knowledge gaps have been filled. CE2 is a transient response, time-at-temperature study for loss-of-forced-circulation (LOFC) transients, both with and without scram (ATWS). The purpose is to determine the time the system remains above a certain temperature threshold during a LOFC transient in the FHR, both with or without a full scram occurring. The significance will be the ability to address the LBE initiating event, "decrease in reactor coolant system flow rate," and that the data can be used to address the limiting safety cases of structural integrity during transients. The experimental facility used in this exercise is the CIET facility (UCB) and the figures of merit include the peak bulk coolant outlet temperature, the time at temperature for metallic and ceramic structures, the temperature difference across the DRACS, and the time to establishment of natural circulation.

These are again the two examples given here. The rational for choosing these holds and is the best path forward for this benchmarking campaign. However, the structure and cooperation of the benchmarking campaign participants has changed and will be explored further in Chapter 6.

5 Additional Concerns for FHR Thermal Hydraulics and Benchmarking

Some issues which came up during the workshop are methods for assessing benchmark completeness and determination of which codes need to benchmarked. A comment was made that a system seems to already be in place for assessing benchmark completeness. Determination of necessary code benchmarks will need to be informed by a combination of code assessment including capability and availability with information regarding licensing strategy and commercial cooperation.

Another concern which arose was the conflict with benchmarking using data from an experiment that may involve proprietary data. In order to work with a vendor that does this, the IRP members need to create enough interest that the vendor wants to create the benchmark.

5.1 Similitude for Coolants

Thermal hydraulic phenomena associated with FHR response to transients significant to reactor safety and performance evolve over short time periods of minutes to days. Therefore, the major constraint on FHR thermal hydraulic experiments is not duration, but instead power and physical scale because of the impracticality of performing thermal hydraulic experiments at the full-power levels of commercial reactors. The ability to use simulant fluids in scaled experiments to replicate molten salt system performance at reduced geometric scale, temperatures, and input powers is a significant development in molten salt thermal hydraulics and allows for the construction of laboratory-scale experiments that produce high quality data valuable for understanding of and technology development for FHRs.

UCB has identified a class of heat transfer oils that match the Prandtl (Pr), Reynolds (Re), and Grashof (Gr) numbers of the major molten salts simultaneously, at approximately 50% geometric scale, temperatures between 50-120°C, and heater power under 2% of prototypical conditions [24]. Dowtherm A, a heat transfer oil in this identified class, is a eutectic mixture of two thermally stable compounds, biphenyl (C12H10) and diphenyl oxide ($C_{12}H_{10}O$). The manufacturer, Dow Chemical, recommends using this fluid in the temperature range between 15°C and 400°C. Combined with its remarkable thermophysical properties to simulate convective heat transfer in fluoride salt systems, its high stability makes Dowtherm A an ideal candidate for scaled experiments. Several distortions using this scaling methodology and Dowtherm A as a simulant fluid do exist: (1) small distortions in length, velocity, and temperature difference scaling at different simulant fluid temperature complicate the selection of static experiment design parameters for use over a range of experimental conditions, (2) thermal radiation is not captured in this scaling methodology; more work is needed to characterize the importance of thermal radiation in molten salts, and careful consideration should be given for each experimental situation to determine the importance of thermal radiation (more important in laminar flow than turbulent), (3) there is a mismatch in length scaling in reduced height vs. reduced area due to buying off-the-shelf piping (volume scaling is thus difficult to match), and (4) currently available and used structural materials in actual models do not follow the same scaling relationship as flibe-to-Dowtherm. Overall, Dowtherm A is an excellent simulant fluid for several candidate molten-salt-coolants, most importantly for flibe, the reference coolant for the Mk1 PB-FHR. Dowtherm A is able to be used as a simulant fluid for flibe through the entire temperature space used by prototypical FHRs with little distortion. This leads to the ability to design and build integral effects test (IET) and separate effects test (SET) facilities utilizing Dowtherm A as a simulant fluid to study molten salt thermal hydraulic phenomena across the full temperature range of prototypical FHRs.

5.2 Similitude for Structural Materials

The same scaling methodology used to identify Dowtherm A as an excellent simulant fluid for flibe in FHR conditions can be used to identify structural materials to simulant metallic structural elements and graphite structures in FHR conditions [30]. However, less work in this area has been done than in studying and using Dowtherm A. It may be possible to use a bronze-loaded PTFE foam that has specific amounts of bronze loading and voids (air pockets in foam) to create the necessary scaled volumetric heat capacity and thermal conduction coefficient.

Designing an experimental facility (SET and/or IET) that uses a combination of Dowtherm A and a simulant structural material may open up a wide and powerful array of experiments that replicate coupled solid-fluid heat transfer in FHRs, which is expected to be the thermal hydraulic phenomenon of most concern due to thermal limits of structural materials in off-normal scenarios, such as LOFC accidents.

5.3 Verification, Validation, and Uncertainty Quantification

Verification, validation, and uncertainty quantification (VVUQ) is the fundamental process of benchmarking. VVUQ must be conducted in order to both qualify and quantify usefulness for simulation data by comparing it with experimental data. Collaboration between IRP members is important for VVUQ as it establishes confidences in individual results as well as the benchmarking results for the entire IRP.

Questions that were discussed during the workshop include the standardization of a VVUQ methodology between IRP members and working groups as well as a comparison with industry best practices. One example comes from Westinghouse, in that benchmarking is for testing code capabilities and not the details of design.

Furthermore, the IRP members must ascertain the requirements needed to establish the success of VVUQ, particularly in the eyes of licensing agencies such as the Nuclear Regulatory Commission.

Finally, as in other topics discussed during the workshop, the role of PIRTs should also be evaluated with respect to VVUQ.

5.4 Conjugate Heat Transfer

As suggested in Section 5.2, heat transfer between solid structural elements (graphite reflector blocks, reactor vessel walls, core inlet and outlet piping, etc.) and fluids (flibe, cover gases), defined as conjugate heat transfer (CHT) will be one of the critical thermal hydraulic phenomena to study, understand, and capture in system models for FHRs. Initial efforts have been made in this area in the construction of system models in codes like RELAP5-3D, and many existing experiments (SETs and IETs) may be able to study this phenomenon with only small additions to existing instrumentation.

5.5 Radiation Heat Transfer

The TCHX is situated outside of the reactor containment vessel and it connects the DRACS salt loop to the water thermosiphon loop. Due to the high temperature differences present in the TCHX between water (100°C) and salt (608-526°C), radiative heat transfer is significant compared to natural convection. According to the simple thermal calculations, the ratio of the radiative heat transfer thermal resistance to the convective heat transfer thermal resistance for a laminar flow in a single tube is considerably larger than 1: $R_{rad}/R_{conv} \cong 6$. The TCHX is designed to have radiation-dominated salt-to-water heat transfer to reduce the likelihood of freezing in the heat exchanger. To better understand radiative heat transfer, the distinction between solid and liquid radiative heat transfer needs to be explored.

In order to model these effects, the surface emissivity of materials immersed in the salt and of frozen FLiBe surface need to be known and the absorptivity of the liquid salt in the infrared needs to be measured. Additional experiments will also be needed to understand the effect of thermal radiation on convection.

Furthermore, the scaling distortions between FLiBe and FLiNaK, which is a commonly used TH simulant, need to be quantified; hence the need for the same measurements in FLiNaK as well.

The radiative heat transfer which will take place in the FHR will be governed by the radiative heat transfer equations given in Figure 36.

$$\Omega \cdot \nabla I(\Omega, s) = \kappa I_b(T) - \beta I(\Omega, s) + \frac{\sigma_s}{4\pi}\int_0^{4\pi} I(\Omega, s)\phi(\Omega', \Omega)\partial\Omega'$$

where

- $I(\Omega, s)$ is the radiative intensity at the position s position in the Ω direction
- T is the temperature
- κ, β, σ_s are absorption, extinction, and scattering coefficients, respectively
- $I_b(T) = \frac{n^2\sigma T^4}{\pi}$ is the blackbody radiation intensity and n is the refractive index

Figure 36. Radiative heat transfer equation with defined parameters from the COMSOL Multiphysics User Guide.

To solve this equation, we need to find the above absorption and scattering coefficients and refractive index of flibe or flinak. The extinction coefficient is merely the sum of the absorption and scattering coefficients. For our purposes the scattering coefficient will be assumed to be zero. It should be noted that these parameters are mean values, and are not wavelength dependent.

We are looking into purchasing an FTIR accessory which will allow for high temperature in-situ study of molten salt spectra. Using this device we can measure the coefficient of reflectivity, r, as function of wavelength for a molten salt species. Then, using the Kramer's-Koenig transformation of the reflectance, we can derive the extinction index, k and the refractive index, n, [27]. We can then calculate k, the absorption coefficient using the following relation, where λ is wavelength of incident light.

$$\mathrm{k} = \frac{4\pi k}{\lambda}$$

Finally, we obtain the mean absorption coefficient by integrating the wavelength dependent absorption coefficient multiplied by the Planck Distribution, and dividing this product by the energy emitted by a blackbody at temperature, T. A similar integration can be done to obtain the mean refractive index.

5.6 Salt Freezing

Natural circulation emergency cooling systems with FLiBe as the working fluid are potentially vulnerable to overcooling, especially if the plant loses trace heater power. For this reason, it is important to develop predictive capability for transient response with freezing and melting.

There are other freezing action items that need to be addressed. Because of freezing being potentially catastrophic in the TCHX, consideration must be given to salt flow in the shell side of the heat exchanger. This may allow salt to bypass the freezing blockage more easily than in a pipe flow. This also allows the heat exchanger pipes to better withstand mechanical forces caused by freezing of the salt. Double walls would still be required to ensure heat transfer is predominantly radiative, which theoretically helps prevent salt freezing and makes recovery more likely in the TCHX. In order to study this concept, a version of the Static Freezing Experiment which is reversed to be a cold finger insertion should be conducted. The effect of radiative heating on freezing initiation and recovery needs to be explored. In general, the effect of salt freezing on heat exchanger effectiveness needs characterization.

If freezing occurs in a heat exchanger, partial or total pipe blockage will initiate. It is important to understand the positive and the negative feedback response of the system to freezing, and to develop system-level modeling capability for overcooling transients that include freezing.

In water, studies have shown that supercooling can lead to dendritic freezing, which then leads to the formation of a slurry and eventual pipe blockage; otherwise a freezing front growth from the heat exchange surface is observed, which has a feedback effect on convective heat transport, and leads to a continuously evolving frozen layer, and a transient pressure drop and convective heat transfer coefficient [28]. Based on these studies with water, we understand that supercooling can play a role in the evolution of heat transfer and pressure drop coefficients during freezing transients. Supercooling is a statistical process that depends on environmental conditions, fluid properties, and solid surface properties. Unlike a deterministic process, under identical macroscopic conditions, the degree of supercooling will not be identical for repeated experimental runs; rather, there is a probability distribution for initiation of nucleation. This phenomenon needs to be characterized for FLiBe and its surrogate fluids (such as FLiNaK) as well as its simulant fluids (such as Dowtherm A).

Furthermore, with water and long heat exchanger pipes, Gilpin has shown that there are regimes in which the frozen layer forms a wave-like pattern, with thin and thick frozen regions, and that the waves move in time. According to Gilpin's correlation for water, FHR heat exchangers fall in the wave-regime [28]. This will need to be verified experimentally and computationally for the salts. In this regime, important thermal gradients and pipe thermal stresses may be generated.

By contrast with water, FLiBe is a high Prandtl number fluid, has a much stronger viscosity dependence with temperature around the melting point, has a different volume change upon freezing, and radiative heat transport may play a role. Table 6 summaries the different physical properties and parameters of FLiBe and water at/near their melting points.

Table 6. Comparison between physical properties and parameters of FLiBe and water at/near their melting points.

Parameter	FLiBE at 459°C	Water at 0°C	Unit
Prandtl Number	42	14	-
Viscosity	0.017	0.0018	kg/m-s
Coefficient of Thermal Expansion	2.4E-4	0.5E-4	1/K
Liquid Specific Heat/Solid Specific Heat	1	2	-
Liquid thermal conductivity/Solid thermal conductivity	1	0.3	-

Radiative heat transport may play a role in characterization of freezing phenomenology. The local temperature and flow profiles may be sensitive to radiative heat transport between pipe walls and frozen FLiBe, as well as by absorption in the liquid, as a participating media. For example, in laminar flow of salt, which is expected in heat exchangers of passive safety systems, there can be a more significant profile in the coolant than in a forced, turbulent flow of salt. Emission and re-absorption of radiation within the salt would somewhat flatten this profile, which has an effect on the potential onset of freeze front propagation from the pipe boundary.

In summary, in order to predict the evolution of transients that include freezing, the following research questions need to be addressed:

1. Experimental studies of supercooling and freezing regimes for FLiBe, and its surrogate and simulant fluids.

2. Development of fluid-dynamics models capable of predicting freezing front propagation, and the evolution of convective heat transport and pressure drop. The initial geometry of interest is flow in a heat exchanger pipe. Capability to include the effect of radiative heat transport is important.

3. Development of system thermal-hydraulic codes that incorporate 1-D models of freezing and melting.
4. IETs that include freezing, for the validation of the 1-D thermal-hydraulic codes.
5. Identification of simulant fluids that can be used for solidification studies and IETs and SETs that demonstrate the similitude.

5.7 Salt-to-Salt Heat Exchange

Table 7 summarizes some of the concerns presented above as well as some additional concerns associated with salt heat transfer and some actions currently underway or required to help address these concerns.

Table 7. Salt-to-salt heat exchange phenomena, concerns, and approaches.

Phenomenon	Concerns	What is being/could be done?
Similitude for coolants	Limitations to similitude between Dowtherm A/flibe including freezing and thermal radiation	Cartridge Heater Experiment at UCB to assess natural circulation similitude Freezing work at UW will help assess freezing similitude More information is needed about thermal radiation in impure flibe
Similitude for structural materials	Structural responses of concern during some transients, and relatively less work has focuses on structural similitude	Additional experimental efforts investigating structural similitude
VVUQ	In addition to the need for across-the-board VVUQ efforts, large uncertainties are present in thermophysical properties of some salts (for one assessment, see [31])	Need to broad adoption of VVUQ in post-processing of experimental and simulation data Characterization program for salts of interest in FHR design
Conjugate heat transfer	Understanding structural/fluid heat transfer will be critical to predicting thermal transients in the FHR	Many available experiments and modeling tools may be utilized to help better understand conjugate heat transfer with potentially small instrumentation upgrades

Radiative heat transfer	Salt participating medium properties not well understood	More experimental information is needed about thermal radiation in impure flibe
Freezing	Localized freezing anticipated in some long-term transients Full freezing possible Effect of freeze/thaw cycling on structure integrity and material degradation	Experimental program underway on freezing behavior of salts pertinent to FHR design
Corrosion	Long-term corrosion of flowing salts on structural materials unknown Effect on corrosion due to presence of graphite, sparging gases, and tritium getters on structural materials unknown	Experimental program underway on corrosion behavior and chemistry control for salts flowing by forced and natural convection on structural materials of interest for the FHR
Chemical hazards	Presence of beryllium in some salts	Experimental program studying freezing of flibe help develop beryllium expertise
Radiological hazards	Tritium getters in some double-wall heat exchanger designs may lead to large radiological inventories	Modeling work on tritium transport and retention and heat exchanger performance will provide better tools

5.8 Computational Fluid Dynamics (CFD)

The values and limitations of computational fluid dynamics (CFD) need to be evaluated as they are applied to separate effects tests, integral effects tests, simulations, and all benchmarking activities.

5.9 Liquid-Fuel Reactor Phenomena

There are some similarities between solid-fuel and liquid-fuel molten salt reactors which may allow for parallel technology development and provide incentives for communication and information exchange. Due to the potential for an increased pool of benchmarking resources, the IRP members discusses similarities and differences between liquid-fuel and solid-fuel molten salt reactors in areas including reactor physics, thermal-hydraulics, chemistry and materials, and other design issues.

With respect to reactor physics, liquid-fuel reactors must be treated differently due to the contrast between homogeneous fuel/coolant configurations and solid-fuel designs with double heterogeneity such as TRISO particles embedded in a graphite pebble matrix. There are other concerns associated with drift of delayed neutron precursors and methods for fission product removal during burnup.

For a comparison of thermal-hydraulics characteristics between liquid-fuel and solid-fuel molten salt reactors, the understanding of the intrinsic coupling between reactor physics and thermal-hydraulics in liquid-fuel reactors is paramount to their design. Some key phenomena will be fission heat deposition in the fuel and coolant and the effects of a distributed decay heat source.

There are some similarities between solid-fuel and liquid-fuel reactors with regards to chemistry and materials. Fission products in the coolant will be a common issue for both classes of reactor, although significantly more so for liquid-fuel reactors. Both reactors will have similar issues with respect to tritium generation.

Additional issues include the effects of fast fission radiation damage and the resulting shielding requirements at the reactor walls. More specific to liquid-fuel reactors is neutron production in the primary coolant path beyond the core. One tradeoff that is currently unclear is the separation of fission products from the primary system, which helps to shrink the source term but with currently undetermined consequences. Finally, the role of online monitoring and service inspection remains to be determined.

6 Working Group Structure and Path Forward

Moving forward, communication and collaboration is necessary among the partners within the THWG to achieve the benchmarking goals of this FHR IRP. The structure of the working group and a proposed path forward is presented below.

6.1 Structure

The structure of the THWG is still under development, but several important decisions were made during the workshop:

- Working Group Chairs: Prof. Per Peterson (UCB) and Prof. Xiaodong Sun (OSU)
- Advisory Board members:
    - Prof. Emilio Baglietto (MIT)
    - Prof. Ed Blandford (UNM)
    - Prof. Lin-wen Hu (MIT)
    - Dr. Chong Zhou (SINAP)
    - More to be determined

Additional advisory board members are needed. A suggestion during the workshop was to have representation from each IRP partner as well as significant partners outside the IRP, such as the national laboratories (ANL, INL, and ORNL) as well as SINAP. A further suggestion is to identify subject matter experts to be included in the advisory panel, including experts in reactor licensing and commercialization.

Further working group structural details that need clarification include:

- Which universities/labs/students are assigned to which task
- How often does communication occur within the working group
- What are the working group's timeline and deliverables
- Should this benchmarking campaign be integrated with OECD/NEA

The structure of the working group will need to be captured in a Working Group Charter after the necessary details are determined.

6.2 Path Forward

The path forward for the THWG is somewhat predicated on the structure and major structural decisions that will be captured in the charter, but several important items to note were discussed during the workshop:

- An information repository for experiment results, experiment procedures, model predictions, model inputs, model nodalizations, best practices, and corrective actions that can be shared among all participants as well as provide a secure location to house information deemed important (legacy data) is necessary; information repositories identified for consideration include NE-KAMS (ORNL) and GitHub
- A list of code options is important to maintain that may include:
    - RELAP5-3D
    - RELAP5/SCADAPSIM/MOD 4.0
    - RELAP-7
    - TRACE
    - Flownex
    - SAM (INL thermal hydraulics system code)
- Identify benchmark problems of interest (two examples have been identified in this workshop as well as the previous workshop, but more specific problems need to be agreed upon)
- An overall goal should be explicitly agreed upon so all participants are working to the same end; the goal tentatively set forth in the workshop is: get a system that works (model to use, property data to use, communication and repository methods to use, etc.)
- IET and SET sessions for benchmarking updates and results should be scheduled for the upcoming NURETH-17 conference (September 2017)

Here again, much work is needed in clarifying details relevant to performing benchmark exercises. Much of this clarification is predicated on the details of the Working Group Charter which is still being developed.

A conclusion in retrospect has been that while this working group enjoys a plethora of available experiments, models, and willing students, there is very little IRP cohesion and motivation to collaborate as all participants already have much individual work already laid out. However, all individual work is still incredibly important and helpful to the overall goals of this working group as well as the IRP at large. It is suggested here that a balance be struck between the individual goals of the participants in this benchmarking campaign as well as the tasks in the benchmarking campaign itself. If these two efforts (individual research vs. benchmarking efforts) can be aligned, all the better.

7 References

[1] C. W. Forsberg, "Molten-salt-cooled advanced high-temperature reactor for production of hydrogen and electricity," *Nucl. Technol.*, vol. 144, pp. 289-30, 2003.

[2] U.S. Nuclear Regulatory Commission, "Regulatory Guide 1.203: Transient and Accident Analysis Methods," 2005.

[3] F. Carotti, M. A. Dbai, K. Ahmed, and R. O. Scarlat, "Experimental and Modeling Studies of Over-Cooling Transients in Fluoride-Salt Cooled High-Temperature Reactors," in *Proceedings of the International Topical Meeting on Nuclear Rector Thermalhydraulics (NURETH-16)*, 2015, pp. 6169–6182.

[4] L. J. Chapdelaine, K. K. Ahmed, M. A. Dbai, and R. O. Scarlat, "Experimental and Computational Study of Fluoride Salt Mixture Solidification," in *International Congress on Advances in Nuclear Power Plants (ICAPP 2016)*, 2016.

[5] H. C. Lin et al., "RELAP5 model validation and benchmark for DRACS thermal performance," presented at the *International Congress on Advances in Nuclear Power Plants (ICAPP)*, San Francisco, CA, 2016.

[6] C. Davis, "Implementation of molten salt properties into RELAP5-3D/ATHENA," Idaho National Laboratory, Idaho Falls, ID, Rep. INEEL/EXT-05-02658, 2005.

[7] D. Williams, "Assessment of candidate molten salt coolants for the NGNP/NHI heat transfer loop," Oak Ridge National Laboratory, Oak Ridge, TN, Rep. ORNL/TM-2006/69, 2006.

[8] N.A. Anderson and P. Sabharwall, "Molten salt mixture properties (KF-ZrF_4 and KCl-$MgCl_2$) for use in RELAP5-3D for high-temperature reactor application," *Nucl. Technology*, vol. 178, no. 3, pp.335-340, June, 2012.

[9] W.D. Powers, S.I. Cohen, and N.D. Greene, "Physical properties of molten reactor fuels and coolants," *Nucl. Science and Engineering*, vol. 17, no. 2, pp. 200-211, Oct., 1963.

[10] S. Cantor, J. Cooke, A. Dworkin, G. Robbins, R. Thoma, and G. Watson, "Physical properties of molten-salt reactor fuel, coolant, and flush salts," Oak Ridge National Laboratory, Oak Ridge, TN, Rep. ORNL/TM-2316, 1968.

[11] G.J. Janz, "Thermodynamic and transport properties for molten salts: correlation equations for critically evaluated density, surface tension, electrical conductance, and viscosity data," *J. Phys. Chem. Ref. Data*, vol. 17, suppl. 2, 1988.

[12] Q. Lv, X. Wang, I.H. Kim, X. Sun, R.N. Christensen, T.E. Blue, G. Yoder, D. Wilson, and P. Sabharwall, "Scaling analysis for the direct reactor auxiliary cooling system for FHRs," *Nucl. Engineering and Design*, vol. 285, pp. 197-206, April, 2015.

[13] Q. Lv, X. Wang, I. Adams, X. Sun, R.N. Christensen, T.E. Blue, G. Yoder, D. Wilson, and P. Sabharwall, "Scaling analysis for the direct reactor auxiliary cooling system for AHTRs," presented at the *15th International Topical Meeting on Nuclear Reactor Thermal Hydraulics (NURETH-15)*, Pisa, Italy, 2013.

[14] B. V. Dzyubenko, L. –V. A. Ashmantas, and M. D. Segal, *Modeling and Design of Twisted Tube Heat Exchangers*, Danbury, CT: Begell House, 2000.

[15] J. T. Hughes and E. D. Blandford, "Experimental Investigation of a Directionally Enhanced DHX Concept for High Temperature Direct Reactor Auxiliary Cooling Systems," *Nucl. Eng. and Design*, Vol. 303, pp. 132-152, July, 2016.

[16] "Fluoride-salt-cooled, high-temperature reactor code benchmarking white paper,"

University of California Berkeley, Berkeley, CA, Rep. UCBTH-15-001, 2015.
[17] "Argonne liquid-metal advanced burner reactor – components and in-vessel system thermal-hydraulic research and testing experience pathway forward," Argonne National Laboratory, Argonne, IL, Rep. ANL/NE-07/21, 2007.
[18] United States Nuclear Regulatory Commission. (2015, October 9). *Computer codes* [Online]. Available: http://www.nrc.gov/about-nrc/regulatory/research/safetycodes.html
[19] Z. Duan, F. Shen, X. Cao, and J. Zhang, "Comprehensive effects of baffle configuration on the performance of heat exchanger with helical baffles," *Nucl. Eng. and Design*, vol. 300, pp. 349-357, April, 2016.
[20] J. –F. WYang, M. Zeng, and Q. –W. Wang, "Effects of sealing strips on shell-side flow and heat transfer performance of a heat exchanger with helical baffles," *Applied Thermal Eng.*, vol. 64, no. 1-2, pp. 117-128, March, 2014.
[21] E. Pal, I. Kumar, J. B. Joshi, and N. K. Maheshwari, "CFD simulations of shell-side flow in a shell-and-tube type heat exchanger with and without baffles," *Chem. Eng. Sci.*, vol. 143, pp. 314-340, April, 2016.
[22] K. B. Welter et al., "APEX-AP1000 confirmatory testing to support AP1000 design certification," U.S. NRC, Washington, DC, Rep. NUREG-1826, 2005.
[23] N. Zweibaum et al., "Design of the compact integral effects test facility and validation of best estimate models for fluoride-salt-cooled, high-temperature reactors," *Nucl. Technology*, to be published.
[24] X. Wang, Q. Lv, X. Sun, R.N. Christensen, T.E. Blue, G. Yoder, D. Wilson, and P. Sabharwall, "A modular design of a direct reactor auxiliary cooling system for AHTRs," in *American Nuclear Society 2011 Annual Meeting*, Hollywood, FL, 2011, pp. 1077-1080.
[25] Q. Lv, H.C. Lin, X. Sun, R.N. Christensen, T.E. Blue, G. Yoder, D. Wilson, and P. Sabharwall, "Experimental study of DRACS thermal performance in a low-temperature test facility," presented at the *16th International Topical Meeting on Nuclear Reactor Thermal Hydraulics (NURETH-16)*, Chicago, IL, 2015.
[26] Q. Lv, H.C. Lin, I.H. Kim, X. Sun, R.N. Christensen, T.E. Blue, G. Yoder, D. Wilson, and P. Sabharwall, "DRACS thermal performance evaluation for FHR," *Annals of Nuclear Energy*, vol. 77, pp. 115-128, Nov., 2014.
[27] J. K. Wilmshurst and S. Senderoff, "Vibrational Spectra of Inorganic Molecules. IV. Infrared Reflection Spectra of Liquid Lithium, Sodium, Potassium and Silver Nitrates," *J. Chem. Phys.*, vol. 35, no. 3, p. 1078, 1961.
[28] R. R. Gilpin, "Ice Formation in a Pipe Containing Flows in the Transition and Turbulent Regimes," *J. Heat Transfer*, vol. 103, no. May 1981, pp. 363–369, 1981.
[29] Q. Lv, M. Chen, I.H. Kim, X. Sun, R.N. Christensen, T.E. Blue, G. Yoder, D. Wilson, and P. Sabharwall, "Design of fluidic diode for a high-temperature DRACS test facility," presented at the *21st International Conference on Nuclear Engineering (ICONE21)*, Chengdu, China, 2013.
[30] P. M. Bardet and P. F. Peterson, "Options for scaled experiments for high temperature liquid salt and helium fluid mechanics and convective heat transfer," *Nucl. Technology*, vol. 163, no. 3, pp. 344-357, Sept., 2008.
[31] R. Serrano-Lopez, J. Fradera, and S. Cuesta-Lopez, "Molten salts database for energy applications," *Chem. Eng. and Processing: Process Intensification*, vol. 73, pp. 87-102, Nov., 2013.

Other References:

[32] E. K. Bigg, "The supercooling of water," *Physical Society. Section B,* vol. 66, no. 8, pp. 688, Aug., 1953.

[33] F. B. Cheung and L. Baker, "Transient freezing of liquids in tube flow," *Nucl. Sc. Eng.,* vol. 60, no. 1, pp. 1-9, May, 1976.

[34] R. G. Dorsch and P. T. Hacker, "Photomicrographic investigation of spontaneous freezing temperatures of supercooled water droplets," Natl. AC for Aero. Lewis Flight Prop. Lab, Cleveland, OH, Rep. NACA-TN 2142, 1950.

[35] M. Epstein and F. B. Cheung, "On the prediction of pipe freeze-shut in turbulent flow," *ASME J. of Heat Trans.,* vol. 104, no. 2, pp. 381-384, May, 1982.

[36] J. Levine, "Statistical explanation of spontaneous freezing of water droplets," Natl. AC for Aero. Lewis Flight Prop. Lab, Cleveland, OH, Rep. NACA-TN 2234, 1950.

[37] A. T. M. G. Mostafa, J. M. Eakman, and S. L. Yarbro, "Prediction of heat capacities of solid inorganic salts from group contributions," *Ind. Eng. Chem. Res.*, vol. 35, no. 1, pp. 343-348, Jan., 1996.

[38] K. Nitsch, "Thermal analysis study on water freezing and supercooling," *J. Therm. Anal. Calorim.,* vol. 95, no. 1, pp. 11-14, Jan., 2009.

[39] J. E. Pacheco, J. M. Chavez, and M. E. Ralph, "Investigation of cold filling receiver panels and piping in receiver solar power plants," *J. Sol. Energy Eng.,* vol. 117, no. 4, pp. 282-289, Nov., 1995.

[40] P. F. Peterson et al., "Technical description of the Mark 1 pebble-bed fluoride-salt-cooled high-temperature reactor (PB-FHR) power plant," University of California Berkeley, Berkeley, CA, Rep. UCBTH-14-002, 2014.

[41] R. V. Seeniraj and G. S. Hari, "Transient freezing of liquids in forced flow inside convectively cooled tubes," *Int. Com. Heat Mass Trans.,* vol. 35, no. 6, pp. 786-792, July, 2008.

[42] M. S. Sohal, M. A. Ebner, P. Sabharwall, and P. Shape, "Engineering database of liquid salt thermophysical and thermochemical properties," Idaho National Laboratory, Idaho Falls, ID, Rep. INL/EXT-10-18297, 2010.

[43] P. K. Vijayan, and A. K. Nayak, "Introduction to instabilities in natural circulation systems," The Abdus Salam International Centre for Theoretical Physics, Trieste, Italy, Rep. 2152-22, 2010.

[44] D. F. Williams, L. M. Toth, and K. T. Clarno, "Assessment of candidate molten salt coolants for the advanced high-temperature reactor (AHTR)," Oak Ridge National Laboratory, Oak Ridge, TN, Rep. ORNL/TM-2006/12, 2006.

[45] Q. Wu, and J. J. Sienicki, "Stability analysis on single-phase natural circulation in Argonne lead loop facility," *Nucl. Eng. and Design,* vol. 224, no. 1, pp. 23-32, Sept., 2003.

[46] M. Yamada, M. Tago, S. Fukusako, and A. Horibe, "Melting point and supercooling characteristics of molten salt," *Therma. Acta.*, vol. 218, pp. 401-411, May, 1993.

[47] K. E. Zachariassen, J. H. Lehr, and J. W. W. Keeley, *Water Enclyclopedia,* Hoboken, NJ: Wiley, 2005.